



## Cost analysis of vaccination in tick-mouse transmission of Lyme disease

Daniel Carrera-Pineyro<sup>a</sup>, Harley Hanes<sup>b</sup>, Adam Litzler<sup>c</sup>, Andrea McCormack<sup>d</sup>, Josean Velazquez-Molina<sup>e</sup>, Anuj Mubayi<sup>e</sup>, Karen Ríos-Soto<sup>f</sup>, Christopher Kribs<sup>g,\*</sup>

<sup>a</sup> University of the Incarnate Word, San Antonio, TX, USA

<sup>b</sup> Tulane University, New Orleans, LA, USA

<sup>c</sup> The Ohio State University, Columbus, OH, USA

<sup>d</sup> North Central College, Naperville, IL, USA

<sup>e</sup> Arizona State University, Tempe, AZ, USA

<sup>f</sup> University of Puerto Rico at Mayagüez, Mayagüez, Puerto Rico, USA

<sup>g</sup> The University of Texas at Arlington, Box 19408, Arlington, TX 76019-0408, USA



### ARTICLE INFO

#### Article history:

Received 25 July 2019

Revised 8 March 2020

Accepted 10 March 2020

Available online 10 March 2020

#### Keywords:

Difference equation

*Borrelia burgdorferi*

SI disease model

Host vaccination

### ABSTRACT

Lyme disease is one of the most prevalent and fastest growing vector-borne bacterial illnesses in the United States, with over 25,000 new confirmed cases every year. Humans contract the bacterium *Borrelia burgdorferi* through the bite of the tick *Ixodes scapularis*. The tick can receive the bacterium from a variety of small mammal and bird species, but the white-footed mouse *Peromyscus leucopus* is the primary reservoir in the northeastern United States, especially near human settlement. The tick's life cycle and behavior depend greatly on the season, with different stages of tick biting at different times. Reducing the infection in the tick-mouse cycle may greatly lower human Lyme incidence in some areas. However, research on the effects of various mouse-targeted interventions is limited. One particularly promising method involves administering vaccine pellets to white-footed mice through special bait boxes. In this study, we develop and analyze a mathematical model consisting of a system of nonlinear difference equations to understand the complex transmission dynamics and vector demographics in both tick and mice populations. We evaluate to what extent vaccination of white-footed mice can affect Lyme incidence in *I. scapularis*, and under which conditions this method saves money in preventing Lyme disease. We find that, in areas with high human risk, vaccination can eliminate mouse-tick transmission of *B. burgdorferi* while saving money.

© 2020 Elsevier Ltd. All rights reserved.

## 1. Introduction

*Borrelia burgdorferi*, a bacterial species of spirochete, is the main causative agent of Lyme disease, a tick-borne illness. The bacteria is mainly present in the northeastern United States, as well as in areas of Asia and Europe (Schwartz et al., 2017). In the U.S., there are approximately 30,000 confirmed cases reported to the Centers for Disease Control and Prevention (CDC) every year but actual cases have been estimated as high as 300,000 cases per year (Centers for Disease Control and Prevention, 2018). Symptoms can be debilitating, but may not appear for months after infection (Centers for Disease Control and Prevention 2018).

Lyme disease is transmitted through the bite of hard bodied ticks (Shapiro, 2014). The bacteria cannot be transmitted from parent to offspring in humans by birth or nursing (Mather et al., 1991). Reservoirs of *B. burgdorferi* include small mammals, such as mice, shrews, chipmunks and skunks, as well as some species of birds. The focus of this research is to assess the effectiveness of a new control method for Lyme disease in the U.S.

In eastern North America, the primary Lyme disease vector is the black-legged tick or deer tick, *Ixodes scapularis* (Shapiro, 2014). The vector's two-to-three-year life cycle is segmented into three stages as illustrated in Fig. 2. Ticks feed only three times in their lives, each time taking a blood meal from a host to reach the next developmental life stage (Centers for Disease Control and Prevention 2018). A tick feeds by attaching to a host and drawing blood over a period of three to five days (Minnesota Department of Health, 2018). *B. burgdorferi* can then enter the host

\* Corresponding author.

E-mail address: [kribs@uta.edu](mailto:kribs@uta.edu) (C. Kribs).

through the tick's saliva (or the tick through the blood meal) while the tick feeds for the next 16 to 36 hours (Cook, 2015).

Black-legged ticks are born uninfected as larvae in the spring. In the summer, they seek a blood meal from any sort of small mammal, potentially acquiring *B. burgdorferi* if the host is infected. After molting to the nymphal stage, they next feed the following spring. Nymphs feed on any size mammal, from mice to deer to humans (Minnesota Department of Health, 2018). This is where human risk is the greatest since nymphs are transparent in color and only about 2 mm in length, making them difficult to detect on the body. If the tick had previously become infected in the larval stage it can then, as a nymph, infect its host. After molting again, they reach the adult stage that fall and seek a final blood meal. In the adult stage they prefer large mammals such as white tailed deer. Having completed their final blood meal in the fall, the adults mate, lay eggs, and then shortly die (Lane et al., 1991).

Although ticks will feed on a variety of hosts, of particular importance to the persistence of *B. burgdorferi* is the white-footed mouse *Peromyscus leucopus*. White-footed mice are the preferred biting targets of larval ticks and are often targeted by nymphs as well. These mice are generalists and live in a variety of habitats in eastern North America, thriving especially in habitats where their natural predators are absent, such as fragmented forests near suburban human settlements (Way and White, 2013; LoGiudice et al., 2003). *P. leucopus* do not experience any significant reduction in fitness due to either the *B. burgdorferi* bacteria or from feeding by larval and nymphal ticks. An individual mouse commonly becomes infected by a nymphal tick, and goes on to spread the infection to many more larvae over the rest of its one-year life since a mouse may have up to 100 ticks in the larval and nymphal stages feeding on it at the same time (Hersh, 2014). These factors combined have all contributed to the high prevalence of the disease in New England and the Upper Midwest.

It is important to note the seasonality in the tick activity: nymphs are mostly active in the spring, larvae in the summer, adults in the fall, and in the winter all stage activity decreases (Lane et al., 1991). This is due to *I. scapularis*'s greatly sedentary behavior: the ticks thus depend on their hosts as means of transportation. Since mice and deer activity tends to be lower during winter, so do tick bite rates in humans. Ticks in the United States do not have a natural predator, and winter is the only natural control mechanism. The advent of climate change leading to shorter, warmer winters is yet another factor in the proliferation of *I. scapularis* and *B. burgdorferi* throughout a widening range (Ostfeld and Brunner, 2015).

With the increase in tick-borne diseases, much research has been undertaken to model transmission dynamics and understand the impact of control methods (Interlandi, 2018; Jordan et al., 2007; Moreno-Cid and de la Lastra J. M., 2013; Schulze et al., 2017; Schwendinger et al., 2013). Vaccines and acaricide, a poisonous substance for ticks and mites, have been studied as interventions to control transmission of *B. burgdorferi* between ticks and mice. Multiple lab studies have shown vaccines' efficacy in eliciting immune reactions in white-footed mice against *B. burgdorferi*'s OspA surface protein, thereby building resistance to infection (Cornstedt et al., 2017; Izac et al., 2017; Schwendinger et al., 2013). Additionally, field trials of vaccinating white-footed mice by distributing food with *E. coli* presenting *B. burgdorferi*'s OspA was effective at reducing prevalence of *B. burgdorferi* in both mice and nymphal ticks (Richer et al., 2014). A current popular method of administration is the use of bait boxes. Bait boxes are placed along frequented mice zones where the smell of food entices the mice to enter the box and pass through a wick covered in fipronil, a commonly used acaricide, which protects the mice from tick bites for the following 4 to 6 weeks (Schulze et al., 2017). Doping the bait in the boxes also distributes vaccines to the mice (Schulze et al., 2017). Many

of these studies focused on fragmented forest environments, common near areas being developed for human use. Forest fragmentation is a large threat to biodiversity since the area becomes unsuitable to animals with larger ranges, but white-footed mice thrive in this environment, often completely out-competing other species of small mammal (LoGiudice et al., 2003).

Although other control methods such as introduction of predators and regulation of host populations have been proposed, most tick control has proven ineffective (an exception being the fungus *Metarhizium anisopliae*), and control of deer populations has not been shown to have a significant effect in reducing tick-borne diseases (Jordan et al., 2007). In this study we focus on modeling the introduction of orally induced vaccines into mice populations to determine the reduction of infected nymphal ticks and hence reduction in human cases.

The enzootic transmission cycle of *B. burgdorferi* has been widely modeled. Some mathematical models seek to understand the complex life cycle of *I. scapularis* and provide insight on factors affecting its behavior such as climate, host populations, and seasonal population dynamics (Dobson et al., 2011; Ogden et al., 2005; Pugliese and Rosa, 2008). Other models of *B. burgdorferi* transmission have given insight on its reproductive number with mice, the importance of targeting *I. scapularis* larvae, and the ability of *B. burgdorferi* to spread geographically (Wang and Zhao, 2017; Zhang and Zhao, 2013). Our research advances this body of work by using the population parameters and dynamics found in previous models, such as Allan et al. (2003); Nupp and Swihart (1996); Ogden et al. (2007); Randolph (1998), to model not just *B. burgdorferi*'s enzootic transmission, but a leading effort to decrease transmission. This will provide critical insight to public health officials, researchers, and institutions seeking to assess the effectiveness of vaccines before they invest in their implementation, and will also provide additional data to the small body of field trials that have been done.

In this study, we model interacting tick and mouse populations subdivided by infection status and (for ticks) life stage. In the following sections of this report, we develop a system of difference equations to describe annual populations while accounting for their complex life cycle seasonality; then we follow classical qualitative analysis with a cost analysis to compare vaccination costs to the economic impact of cases avoided. Our aim is to model a tick-mouse cycle in a fragmented forest environment in the northeastern United States, where field data are available and where human risk is especially high (Schwartz et al., 2017).

## 2. Methods

### 2.1. Assumptions and definitions

To model tick-mouse infection dynamics, we consider certain assumptions. The first is that mice and ticks mix homogeneously at all stages, and that infection does not affect their behavior or interactions within a given geographical area. While we do account for mice having more contacts with larvae than with nymphs, mouse-tick contact rates are taken to be independent of infection status in both mouse and tick. We also assume that infection with *B. burgdorferi* does not affect mouse birth or death rates, nor tick hatching, death, or biting rates. We assume this because evidence suggests that *B. burgdorferi* does not cause any disease in ticks or white-footed mice, making them an excellent reservoir host (Voordouw et al., 2015). The reproductive fitness of white-footed mice is also unaffected by the presence of the parasitic ticks (Hersh, 2014).

We also assume that infectious mice and ticks remain infectious for the rest of their lives, which is supported by current research on *B. burgdorferi* in *I. scapularis* and *P. leucopus*

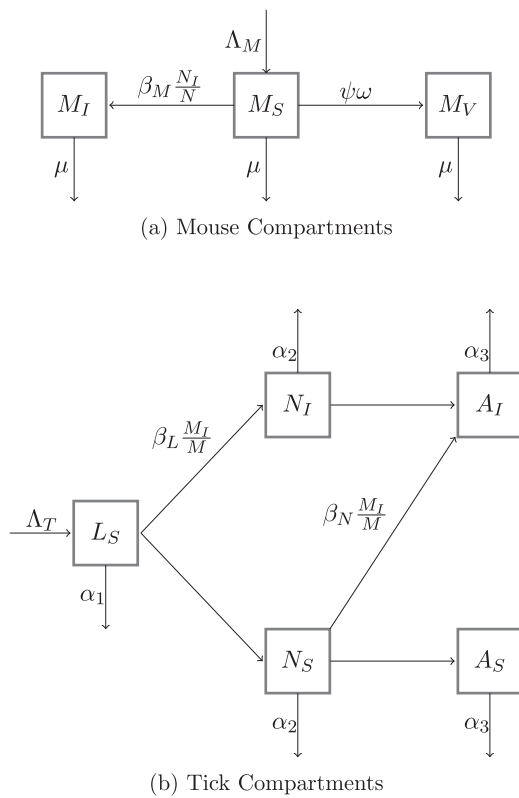


**Fig. 1.** Mouse and tick compartmental model. Rates shown are per capita; transitions without rate labels indicate tick life stage progression over time.

(Barbour and Fish, 1993; Ostfeld and Keesing, 2000; Schwan et al., 1988). We assume that every larva or nymph either dies or successfully feeds to molt before the cohort's next questing season, which is true for the overwhelming majority of ticks (Centers for Disease Control and Prevention, 2018). We adopt this simplifying assumption because the tick life cycle (outlined in Section 2.2) generally allows enough time (outside any winter diapause) to find a host and molt before the next questing period (see Fig. 2). This allows death and molting to be modeled separately: any larva or nymph that does not die before the cohort's next questing period is assumed to progress to nymph or adult, respectively, with the same infection status. Another assumption in this model is that ticks are only infected by mice (and vice versa) since white-footed mice have a very high population density and are larvae's primary hosts (LoGiudice et al., 2003). White-footed mice also transmit and receive *B. burgdorferi* with greater effectiveness than other tick hosts, making them primary spreaders of the pathogen (Barbour et al., 2015). The model incorporates seasonality by having only one life stage of tick feed at a given time. Here, tick questing/feeding periods are mostly divided into two separate seasons although in reality there is some overlap, particularly for nymphs and larvae, which will not be taken into account in this work. The final assumption of our model is that infected ticks and mice do not transmit *B. burgdorferi* to their offspring (Mather et al., 1991; Rosa and Pugliese, 2007).

For our model, we build a system of nonlinear difference equations describing a susceptible, infectious, and vaccinated ( $M_S$ ,  $M_I$ ,  $M_V$ ) mouse population (*P. leucopus*) coupled with a susceptible and infectious ( $N_S$ ,  $N_I$ ) tick population (*I. scapularis*). To understand the mechanisms of these populations, life cycles, and infectiousness, we construct a compartmental diagram representing the system's dynamics, including seasonality. A flow chart capturing the dynamics of the system is shown in Fig. 1, and state variables and model

**Table 1**  
State variables for mice and ticks, taken at time  $t$ .

Variable	Definition
$M(t)$	Total Mouse Population
$M_S(t)$	Susceptible Mice
$M_I(t)$	Infected Mice
$M_V(t)$	Vaccinated Mice
$L_S(t)$	Susceptible Larvae
$N(t)$	Total Nymph Population
$N_I(t)$	Infected Nymphs
$N_S(t)$	Susceptible Nymphs
$A_I(t)$	Infected Adults
$A_S(t)$	Susceptible Adults

**Table 2**  
Parameters for population dynamics.

Parm.	Definition
$\Lambda_M$	Birth/recruitment of mice
$\beta_M$	Transmission constant from nymphs to mice
$\psi$	Contact between mice and vaccines
$\omega$	Proportion of vaccine effectiveness
$\mu$	Natural death of mice
$\Lambda_T$	Recruitment of larvae
$\beta_L$	Transmission constant from mice to larvae
$\beta_N$	Transmission constant from mice to nymphs
$\alpha_1$	Egg to larva natural death
$\alpha_2$	Larva to nymph natural death
$\alpha_3$	Nymph to adult natural death

parameters are summarized in Tables 1 and 2 (units and values are given in Table 3).

Mice have a constant birth  $\Lambda_M$  per generation and a uniform death rate  $\mu$ , with an annual probability of survival thus given by  $e^{-\mu}$ . All mice are born as susceptible, but can then be vaccinated at a rate  $\psi\omega$ , where  $\psi$  is the rate per year at which mice become vaccinated and  $\omega$  the percent effectiveness of the vaccine. If not successfully vaccinated, they become infected by a nymphal tick at rate  $\beta_M \frac{N_I}{N}$ , where  $\beta_M$  is a contact rate (in 1/yr) and  $\frac{N_I}{N}$  gives the infection prevalence of nymphs. The infection rate depends only on nymphs because we assume that larvae do not hatch infected with *B. burgdorferi* so they cannot infect mice when they feed.

Ticks also have a constant recruitment per generation which is defined as  $\Lambda_T$ , being the number of larvae hatching every year. We assume a probability of death as  $e^{-\alpha_i}$ , with each  $\alpha_i$  corresponding to a respective stage change's natural death as in Table 2. A larva becomes infected at rate  $\beta_L \frac{M_I}{M}$ , where  $\beta_L$  gives the rate (in 1/yr) at which a larva has potentially infectious (to the larva) bite contact with mice. Any larva that does not become infected or die at season's end progresses to a susceptible nymph. This transition is based on the assumption that no larvae survive through the next summer without feeding and progressing to nymphs. Nymphs then begin feeding, and susceptible nymphs can be infected at a rate of  $\beta_N \frac{M_I}{M}$ , where  $\beta_N$  denotes the rate (in 1/yr) at which a nymph bites mice multiplied by the proportion of times the bacteria infect a susceptible nymph if it bites an infected mouse. At this point infected nymphs that do not die can also feed on a susceptible mouse to infect it as described for mice above. All infectious nymphs and susceptible nymphs that do not die become infectious and susceptible adults respectively. This transition is based on the assumption that no nymphs survive through the next spring without feeding and progressing to adults.

The infection rates described in the preceding paragraphs can be derived from the common assumption that the vector-host contact rate is proportional to vector density together with the fact (derived formally in Section 3.1) that the host and vector populations are constant from year to year (unaffected by infection).

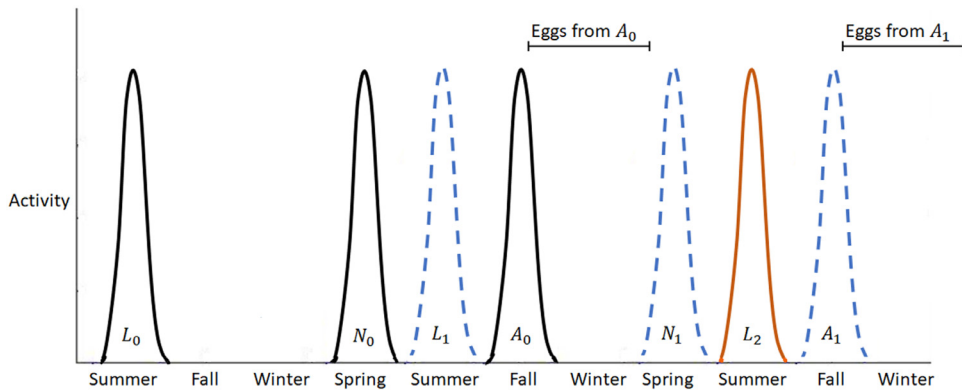


Fig. 2. Two-year tick life cycle with overlapping generations.

**Table 3**  
Parameter values for mouse and tick population dynamics.

Parameter	Definition	Value	Units	Reference
$M_\infty$	Total mouse population	50	mice	(Nupp and Swihart, 1996)
$\Lambda_M$	Birth/recruitment of mice	65.02	mice	
$\psi$	Contact between mice and vaccines	varied	1/year	
$\beta_M$	Transmission constant from nymphs to mice	varied	1/year	
$\omega$	Proportion of vaccine effectiveness	0.96	—	(Schwendinger et al., 2013)
$\mu$	Natural death rate of mice	4.38	1/year	(Ogden et al., 2007; Wang and Zhao, 2017)
$N_\infty$	Total nymph population	1000	ticks	(Allan et al., 2003)
$\Lambda_T$	Recruitment of larvae	$1.998 \times 10^5$	ticks	
$\beta_L$	Transmission constant from mice to larvae	varied	1/year	
$\beta_N$	Transmission constant from mice to nymphs	varied	1/year	
$\alpha_1$	Egg to larva natural death	11.98	1/year	(Randolph, 1998)
$\alpha_2$	Larva to nymph natural death	3.07	1/year	(Randolph, 1998)
$\alpha_3$	Nymph adult natural death	3.22	1/year	(Randolph, 1998)

Assuming (consistent with observation) that vectors (here, tick nymphs) can bite hosts (mice) as often as desired, the overall rate of potentially infectious contacts can be given by  $\beta N$ . Further assuming that these contacts are unaffected by host or vector infection status, a fraction  $M_S/M$  involve uninfected mice, and a fraction  $N_I/N$  involve infected nymphs, so the overall rate of new host infections is  $\beta N \frac{M_S}{M} \frac{N_I}{N}$ . To simplify units, we rewrite this as  $(\beta_M^N) \frac{N_I}{N} M_S$  and, since  $N$  and  $M$  are constant, define  $\beta_M = \beta_M^N$ , leading to the infection rates given in the foregoing paragraphs, and to parameters with units of 1/time.

## 2.2. Model development

In order to derive the final model, we first divide a one year time step into several subintervals, with each subinterval describing one specific process in the cycle. After each of the events is mathematically described, they can be chained together to describe the population dynamics from year to year. First, each important event in the system is associated with one or more arrows on the flowchart. The full list of transition equations derived from these events is provided in [Appendix A.1](#).

For a visual representation of how the 2-year tick life cycle fits in to a model with 1-year time steps see [Fig. 2](#). Although there is only one generation and life stage assumed to be questing and feeding at a time, there are 2 generations that overlap each year. Our yearly cycle begins with nymphs in the spring which quest, feed, and begin molting to the adult phase. We then consider the larvae which hatch from the eggs of the previous year's adults and begin questing and feeding in the summer. These larvae will go on to become the next year's nymphs. In the summer those nymphs are dormant while they transition to adulthood and the larvae that hatched in the end of the spring begin questing and feeding. Those

larvae molt during the fall and winter. In the fall, the adults, who were nymphs in the spring, lay the eggs for the next spring.

These building blocks are designed to be modular to allow for a possible different ordering of events. For the purposes of this model, the cycle is taken to begin and end in the spring, which is peak nymph activity. Thus the following sequence of events for the life cycle and transmission dynamics of the populations is considered:

### Spring

#### 1. Mice are vaccinated

Mice are vaccinated at the beginning of our time step because we want to measure the impact of vaccination as protection against nymphal ticks; thus vaccination must take place before nymphal ticks begin questing and feeding in the spring.

#### 2. Susceptible mice become infected

Mice being infected is the first event related to the nymphal feeding season. Larvae infected in the previous year have now progressed to nymphs and can infect mice by taking blood meals.

### Summer

#### 3. Nymphs become adults

Nymphs becoming adults means that the nymph successfully feeds, and from there any of the following may occur:

- Infected nymphs become infected adults (infected nymph potentially infects host)
- Susceptible nymphs can become infected adults
- Susceptible nymphs can become susceptible adults

#### 4. Mice die

Here we account for mouse deaths that happen in the spring, after vaccination and after nymphs have fed. We separate this event from the other event of deaths in mice to account for the

mice that are infected in the spring but do not survive to infect larvae in the summer.

## 5. Mice are born

Here we account for new births in the mice population that happen in the spring after vaccination and the feeding of nymphs. We separate this event from the other event of births in mice so as to maintain a consistent population size after the deaths calculated in the previous step.

## 6. Larvae hatch

Eggs hatch throughout the summer and become larvae. These larvae do not feed until the following spring (see Fig. 2).

## 7. Larvae die

Here we account for larval deaths that occur during the hatching season and while questing. Thus the later steps involving larvae can assume that all remaining larvae successfully feed.

## 8. Larvae feed on mice

Here all remaining larvae successfully feed and become either infected or susceptible nymphs based on whether they feed on an infected mouse and receive the bacteria. In our model, we count these larvae as nymphs immediately after they feed whereas in reality they will not finish molting to nymphs until next spring.

- Susceptible larvae can become susceptible nymphs
- Susceptible larvae can become infected nymphs

## Fall through winter

## 9. Nymphs die

Here we account for all nymphs that died during molting or while questing. Thus the size of our nymph population is representative of the nymphs that successfully feed and progress to adult, rather than counting nymphs that would have died while molting.

- Infected nymphs die
- Susceptible nymphs die

## 10. Mice die

Here we account for death that takes place from the beginning of summer until the end of winter so that our mouse population count is representative of the population at the beginning of spring.

## 11. Mice are born

Here we account for birth that takes place from the beginning of summer until the end of winter so that our expression for mouse population is representative of the population at the beginning of spring.

In Fig. 2, different generations are designated by the subscripts 0, 1, and 2. Generation 0 finishes in fall of the first year, Generation 1 covers the two-year span of the image, and Generation 0's descendants, Generation 2, begin their lives in summer of the second year. The subscripts are not the same as the  $t$ -indexed yearly time steps in the model. The nymphs and adults for a particular year are the same generation of ticks, while the larvae are another. The vertical axis does not depict relative population size, but indicates respective seasons of questing individuals. In our model, the total population of any stage of tick in each year is the same as the total population of the same stage in all other years, which allows us to organize their two-year cycle in one year. This will be shown later in the analysis section.

To construct our system of equations, we use each rate on the flowchart to create an expression for population before and after its associated event, and then proceed by combining those equations into the full system. As an example, consider  $\mu$ , the rate at which mice die. In a discrete-time system, such rates appear within exponents to reflect the proportions of populations making (or not) the corresponding transition during a given time period.

If we integrate to find the total population before and after one year's worth of deaths we get  $M(t+1) = e^{-\mu}M(t)$ . The proportion of mice that survive is  $e^{-\mu}$ . Likewise, the proportion of mice that die is  $1 - e^{-\mu}$ . Thus each exponential term containing a rate has that rate multiplied by 1 year, making the exponent dimensionless. Our time step of one year is subdivided by seasons in order to accurately account for tick life/activity stages; thus some of the exponents are shown to be fractions. For example,  $e^{-3\mu/4}$  represents survival after three out of the four seasons. This use of fractional exponents is used for recruitment, death, vaccination, and contact constants.

To organize this ordering of events we separate the year into 11 sub-timesteps  $\{t + \frac{i}{11} | i = 1, 2, \dots, 11\}$ . These sub-timesteps do not necessarily correspond to a certain interval of time, and often we account for an entire year's worth of a particular process in each sub-step. If we wish to account for processes over only part of the year our proportions will be of the form  $e^{-\zeta/k}$  for arbitrary parameter  $\zeta$  and fraction of the year  $1/k$ . Furthermore, nonlinear terms will reference other state variables in the exponent, which introduces more complexity to the final equations. A full derivation of the system of equations can be found in Appendix A.2.

The final system of Eq. (1), relating populations of mice and nymphs starting and ending during spring, is presented below. Adult and larvae stages are not included in these final populations as larvae have not yet hatched and adults died in the previous fall. However, the intermediate steps contain solutions for each stage at various points in the year.

Let  $M(t) = M_S(t) + M_I(t) + M_V(t)$  and  $N(t) = N_S(t) + N_I(t)$ , the total population of mice and ticks, respectively. Then the system of equations, system (1), is given by:

$$N_I(t+1) = \Lambda_T e^{-\frac{(\alpha_1+3\alpha_2)}{4}} \left( 1 - e^{-\frac{\beta_I}{4} \frac{M_I(t)e^{-\frac{\mu}{4}} + M_S(t)e^{-\frac{\mu}{4}} - \frac{\psi\omega}{4} \left( 1 - e^{-\frac{\beta_M}{2} \frac{N_I(t)}{N(t)}} \right)}{e^{-\frac{\mu}{4}} M(t) + \frac{\Delta M}{4}}} \right), \quad (1a)$$

$$N_S(t+1) = \Lambda_T e^{-\frac{(\alpha_1+3\alpha_2)}{4}} \left( e^{-\frac{\beta_I}{4} \frac{M_I(t)e^{-\frac{\mu}{4}} + M_S(t)e^{-\frac{\mu}{4}} - \frac{\psi\omega}{4} \left( 1 - e^{-\frac{\beta_M}{2} \frac{N_I(t)}{N(t)}} \right)}{e^{-\frac{\mu}{4}} M(t) + \frac{\Delta M}{4}}} \right). \quad (1b)$$

$$M_S(t+1) = M_S(t)e^{-\mu} e^{-\frac{\psi\omega}{4}} e^{-\frac{\beta_M}{2} \frac{N_I(t)}{N(t)}} + \frac{\Delta M}{4} (e^{-\frac{3\mu}{4}} + 3), \quad (1c)$$

$$M_I(t+1) = M_I(t)e^{-\mu} + M_S(t)e^{-\mu} e^{-\frac{\psi\omega}{4}} (1 - e^{-\frac{\beta_M}{2} \frac{N_I(t)}{N(t)}}), \quad (1d)$$

and

$$M_V(t+1) = M_V(t)e^{-\mu} + M_S(t)e^{-\mu} (1 - e^{-\frac{\psi\omega}{4}}). \quad (1e)$$

The number of susceptible mice at time  $t+1$  is equal to the number of susceptible mice that did not die, did not become vaccinated, and did not become infected in the previous year plus the mice that were born—accounting for the fact that mice are born throughout the year by allowing 1/4 to be born before the larvae feeding season and 3/4 to be born after. The number of infected mice at time  $t+1$  is equal to the number of infected mice that did not die plus the number of susceptible mice that became infected and did not die. Likewise, the number of vaccinated mice at time  $t+1$  is equal to the number of vaccinated mice that did not die plus the number of susceptible mice that became vaccinated and did not die.

The number of infected and susceptible nymphs at time  $t+1$  is equal to the number of eggs hatched times the survival rate times

the probability of becoming infected or not becoming infected, respectively. This rate is based on a contact rate times the proportion of all mice which were infected in the previous summer.

### 3. Qualitative analysis

#### 3.1. Equilibrium densities of *I. scapularis* and *P. leucopus*

The total population size of mice can be described by calculating  $M(t+1)$ , the sum of the susceptible, infected, and vaccinated compartments at time  $t+1$ .

$$M(t+1) = M_S(t+1) + M_I(t+1) + M_V(t+1)$$

$$M(t+1) = e^{-\mu} M(t) + \frac{\Lambda_M}{4} e^{-\frac{3\mu}{4}} + \frac{3}{4} \Lambda_M$$

This is a linear difference equation whose solution is:

$$\begin{aligned} M(t) &= M(0)(e^{-\mu})^t + \frac{\Lambda_M}{4} (e^{-\frac{3\mu}{4}} + 3) \sum_{j=0}^{t-1} e^{-\mu j} \\ &= M(0)(e^{-\mu})^t + \frac{\Lambda_M}{4} (e^{-\frac{3\mu}{4}} + 3) \left( \frac{1 - (e^{-\mu})^t}{1 - e^{-\mu}} \right) \end{aligned}$$

Since  $\mu$  is a positive constant,  $e^{-\mu}$  is a proportion and  $0 < e^{-\mu} < 1$ . Therefore we define

$$M_\infty = \lim_{t \rightarrow \infty} M(t) = \frac{\Lambda_M}{4} \frac{(e^{-\frac{3\mu}{4}} + 3)}{1 - e^{-\mu}}. \quad (2)$$

This is the mouse population at demographic steady state, and it can also be written as:

$$M_\infty = \frac{\Lambda_M}{4} e^{-3\mu/4} \frac{1}{1 - e^{-\mu}} + \frac{3\Lambda_M}{4} \frac{1}{1 - e^{-\mu}}$$

In biological terms, it is the number of mice born during event 5 of any year that did not die plus the number of mice born during event 11 of any year. Since the mouse-tick system is well established prior to the introduction of any control measures, we henceforth assume that  $M(0) = M_\infty$ , so that  $M(t) = M_\infty$  for all  $t > 0$ .

Similar calculations can be performed on the total nymphal tick population with  $N(t+1)$  equal to the sum of the susceptible and infected tick populations at time  $t$ . In the construction of this model, we assumed that there are no demographic pressures on the population other than the constant birth and death rates, so  $N(t)$  is constant from year to year as well. That is,

$$N(t+1) = N_S(t+1) + N_I(t+1) = \Lambda_T e^{-\frac{(\alpha_1+3\alpha_2)}{4}};$$

thus,  $N(t) = N_\infty = \Lambda_T e^{-\frac{(\alpha_1+3\alpha_2)}{4}}$  for all time  $t$ .

$$J|_{DFE} = \begin{bmatrix} \frac{\beta_M \beta_L}{8} \frac{(3e^{-\frac{\mu}{4}} + e^{-\mu})e^{-\frac{3\mu}{4}} - \frac{\psi\omega}{4}}{(1 - e^{-\mu - \frac{\psi\omega}{4}})} & e^{-\mu} \frac{e^{-\frac{(\alpha_1+3\alpha_2)}{4}} (1 - e^{-\mu}) \beta_L \Lambda_T}{(3e^{-\mu} + e^{-3\mu/4}) \Lambda_M} & 0 \\ \frac{\beta_M \Lambda_M}{8 \Lambda_T} \frac{(3e^{-\frac{\mu}{4}} + e^{-\mu})e^{-\frac{3\mu}{4}} - \frac{\psi\omega}{4}}{(1 - e^{-\mu - \frac{\psi\omega}{4}})} & e^{-\mu} & 0 \\ 0 & -e^{-\mu} \left( 1 - e^{-\frac{\psi\omega}{4}} \right) & e^{-\mu - \frac{\psi\omega}{4}} \end{bmatrix}.$$

The total nymph population is equal to the number of hatched eggs times the proportion of nymphs that do survive before the sampling time. It follows from this calculation of  $M_\infty$  and  $N_\infty$  that we can reduce system (1) to a system of three equations. Let  $M_S(t) = M_\infty - (M_I(t) + M_V(t))$  and  $N_S(t) = N_\infty - N_I(t)$ . The system becomes system (3), which is only in terms of the  $N_I$ ,  $M_I$ , and  $M_V$  populations. System (3) will be used throughout the rest of the paper, including in the numerical simulations (Section 4), and is

given by:

$$N_I(t+1) = \Lambda_T e^{-\frac{(\alpha_1+3\alpha_2)}{4}} \left( \frac{\frac{M_I(t)e^{-\frac{\mu}{4}} + (M_\infty - M_I(t) - M_V(t))e^{-\frac{\mu}{4}} - \frac{\psi\omega}{4}}{e^{-\frac{\mu}{4}} M_\infty + \frac{\Lambda_M}{4}} \left( 1 - e^{-\frac{\beta_M}{2} \frac{N_I(t)}{N_\infty}} \right)}{1 - e^{-\frac{\beta_I}{4}}} \right), \quad (3a)$$

$$M_I(t+1) = M_I(t)e^{-\mu} + (M_\infty - M_I(t) - M_V(t))e^{-\mu} e^{-\frac{\psi\omega}{4}} \left( 1 - e^{-\frac{\beta_M}{2} \frac{N_I(t)}{N_\infty}} \right), \text{ and} \quad (3b)$$

$$M_V(t+1) = M_V(t)e^{-\mu} + (M_\infty - M_I(t) - M_V(t))e^{-\mu} \left( 1 - e^{-\frac{\psi\omega}{4}} \right). \quad (3c)$$

In the next section we proceed to calculate the fixed points of system (3) in order to understand its long-term dynamics.

#### 3.2. Disease-free equilibrium

To find fixed points, we start by setting the equations in system (3) equal to their respective populations. That is,  $N_I(t+1) = N_I(t) = N_I^*$ ,  $M_I(t+1) = M_I(t) = M_I^*$ , and  $M_V(t+1) = M_V(t) = M_V^*$ . Setting  $N_I^* = 0$  yields the disease-free equilibrium (DFE),

$$N_S^* = N_\infty, \quad N_I^* = 0, \quad M_S^* = M_\infty \frac{1 - e^{-\mu}}{1 - e^{-\mu - \frac{\psi\omega}{4}}}, \quad M_I^* = 0,$$

$$\text{and } M_V^* = M_\infty \frac{e^{-\mu} (1 - e^{-\frac{\psi\omega}{4}})}{1 - e^{-\mu - \frac{\psi\omega}{4}}}.$$

As expected, the total population is at demographic steady state:  $M_S^* + M_V^* = M_\infty$ . We can also interpret the mouse populations at disease-free equilibrium as proportions of the total equilibrium mouse population. That is,

$$\frac{M_S^*}{M_\infty} = \frac{1 - e^{-\mu}}{1 - e^{-\mu - \frac{\psi\omega}{4}}} \text{ and } \frac{M_V^*}{M_\infty} = \frac{e^{-\mu} (1 - e^{-\frac{\psi\omega}{4}})}{1 - e^{-\mu - \frac{\psi\omega}{4}}}.$$

The expression  $\frac{M_S^*}{M_\infty}$  is the proportion of mice that die, and are thus replaced at demographic equilibrium, over the proportion that either get vaccinated or die. Furthermore,  $\frac{M_V^*}{M_\infty}$  is the proportion that survive times the proportion that do get vaccinated over the proportion that either die or get vaccinated.

The stability of the disease-free equilibrium can be analyzed either via the control reproduction number  $\mathcal{R}_C$  or by linearizing system (3), calculating the Jacobian at the disease-free equilibrium, and identifying the eigenvalues. Notice that this matrix is singular;

the first row is a constant multiple  $\frac{e^{-\frac{(\alpha_1+3\alpha_2)}{4}} (1 - e^{-\mu}) \beta_L \Lambda_T}{(3e^{-\mu} + e^{-3\mu/4}) \Lambda_M}$  of the second. The Jacobian matrix of system (3)  $(N_I, M_I, M_V)$  at the DFE is given by

$$\begin{bmatrix} & & \\ & & \\ & & \\ & & \\ & & \\ & & \end{bmatrix}.$$

The eigenvalues of this matrix are  $\lambda_1 = 0$ ,  $\lambda_2 = e^{-\mu - \frac{\psi\omega}{4}}$ , and  $\lambda_3 = (1 - e^{-\mu})r + e^{-\mu}$ , where

$$r = \frac{\beta_M \beta_L e^{-\frac{\psi\omega}{4}}}{8(1 - e^{-\mu - \frac{\psi\omega}{4}})} \left( \frac{e^{-\mu} + 3e^{-\mu/4}}{1 + 3e^{-\mu/4}} \right). \quad (4)$$

Since  $|\lambda_1| < 1$ ,  $|\lambda_2| < 1$ , the DFE is locally asymptotically stable iff  $|\lambda_3| < 1$ . But  $\lambda_3 > 0$ , and some algebra shows that  $\lambda_3 < 1$  iff  $r < 1$ .

Although  $r < 1$  is a condition for stability,  $r \neq \mathcal{R}_C$ . But by Allen and van den Driessche (2008) either  $r = \mathcal{R}_C = 1$ ,  $1 < r \leq \mathcal{R}_C$ , or  $0 \leq \mathcal{R}_C \leq r < 1$ , meaning stability conditions based on  $r$  are equivalent to stability conditions based on  $\mathcal{R}_C$ . The canonical value of  $\mathcal{R}_C$  can be calculated using the next-generation matrix approach (see Appendix A.4 for details):

$$\mathcal{R}_C = \frac{1}{2} \left( r(1 - e^{-\mu}) + \sqrt{r^2(1 - e^{-\mu})^2 + 4re^{-\mu}} \right). \quad (5)$$

This expression, which gives the average number of secondary infections (of either species) produced by a single infective of the same species introduced into a completely susceptible population, depends on  $\frac{\partial N_I(t+1)}{\partial N_I(t)} = r(1 - e^{-\mu})$  and a term representing  $\frac{\partial N_I(t+1)}{\partial N_I(t)}$  times  $\frac{e^{-\mu}}{1 - e^{-\mu}}$ , the equilibrium proportion of mice that have survived from previous years. By inspection,  $r < 1$  iff  $\mathcal{R}_C < 1$ .

We note that  $\mathcal{R}_0$ , the basic reproduction number, is analogous to  $\mathcal{R}_C$  but defined for a context in which no control method, no vaccination in this case, is introduced into the population. An expression for  $\mathcal{R}_0$  can be derived by setting  $\psi = 0$  in Eq. (5) for  $\mathcal{R}_C$ .

### 3.3. Endemic equilibrium

To determine the existence of further fixed points we reduce the system of equilibrium conditions to one equation. We solve the steady-state version of Eq. (3c) for  $M_V^*$  in terms of  $M_I^*$  and Eq. (3b) for  $M_I^*$  in terms of  $N_I^*$ . Substituting the resulting expressions into Eq. (3a), we can write a single equation in terms of  $N_I^*$ . For the full derivation, see Appendix A.5. Equilibria are then roots of this equation on the interval  $[0,1]$ :

$$G\left(\frac{N_I^*}{N_\infty}\right) = \ln\left(1 - \frac{N_I^*}{N_\infty}\right) + \frac{\beta_L M_\infty e^{-\frac{\mu}{4}} e^{-\frac{\psi\omega}{4}}}{4(e^{-\frac{\mu}{4}} M_\infty + \frac{\Delta_M}{4})} \left( \frac{1 - e^{-\frac{\beta_M}{2} \frac{N_I^*}{N_\infty}}}{1 - e^{-\mu - \frac{\psi\omega}{4}} e^{-\frac{\beta_M}{2} \frac{N_I^*}{N_\infty}}} \right) = 0. \quad (6)$$

Since Eq. (6) is transcendental, we cannot find its zeroes analytically. However, by inspection, we notice that  $G(0) = 0$ , reflecting the existence of the disease-free equilibrium. In addition, there exists a unique endemic equilibrium (a root of  $G$  in  $(0,1)$ ) iff  $\mathcal{R}_C > 1$ , which can be seen as follows. By inspection,  $G(x) \rightarrow -\infty$  as  $x \rightarrow 1^-$ . We calculate

$$G'(x) = -\frac{1}{1-x} + \frac{\beta_L \beta_M M_\infty e^{-\frac{\mu}{4}} e^{-\frac{\psi\omega}{4}}}{8(e^{-\frac{\mu}{4}} M_\infty + \frac{\Delta_M}{4})} \cdot \frac{(1 - e^{-\mu - \frac{\psi\omega}{4}}) e^{-\frac{\beta_M}{2} x}}{(1 - e^{-\mu - \frac{\psi\omega}{4}} e^{-\frac{\beta_M}{2} x})^2}$$

from which

$$G'(0) = \frac{\beta_L \beta_M M_\infty e^{-\frac{\mu}{4}} e^{-\frac{\psi\omega}{4}}}{8(e^{-\frac{\mu}{4}} M_\infty + \frac{\Delta_M}{4})} \cdot \frac{(1 - e^{-\mu - \frac{\psi\omega}{4}})}{(1 - e^{-\mu - \frac{\psi\omega}{4}} e^{-\frac{\beta_M}{2} x})^2} - 1$$

and also

$$G'(x) = 0 \Leftrightarrow 1 - x = \frac{8(e^{-\frac{\mu}{4}} M_\infty + \frac{\Delta_M}{4})}{\beta_L \beta_M M_\infty e^{-\frac{\mu}{4}} e^{-\frac{\psi\omega}{4}}} \cdot \frac{(1 - e^{-\mu - \frac{\psi\omega}{4}} e^{-\frac{\beta_M}{2} x})^2}{(1 - e^{-\mu - \frac{\psi\omega}{4}} e^{-\frac{\beta_M}{2} x})} = h(x).$$

Since some algebra shows that  $h'(x) > 0$ , and thus  $h(x)$  is increasing, while  $1 - x$  is decreasing, the two functions can intersect in at most one point. This occurs iff

$$h(0) = \frac{8(e^{-\frac{\mu}{4}} M_\infty + \frac{\Delta_M}{4})}{\beta_L \beta_M M_\infty e^{-\frac{\mu}{4}} e^{-\frac{\psi\omega}{4}}} \cdot (1 - e^{-\mu - \frac{\psi\omega}{4}}) < 1,$$

which is the same condition as  $G'(0) > 0$  and also (since, from (2),  $\frac{M_\infty e^{-\mu/4}}{M_\infty e^{-\mu/4} + \Delta_M/4} = \frac{e^{-\mu} + 3e^{-\mu/4}}{1 + 3e^{-\mu/4}}$ ) equivalent to  $r > 1$  and thus  $\mathcal{R}_C > 1$ .

Fig. 3 illustrates graphs of  $G$  using three different sets of values for the infection rates  $\beta_M$  and  $\beta_L$ , with other parameter values as

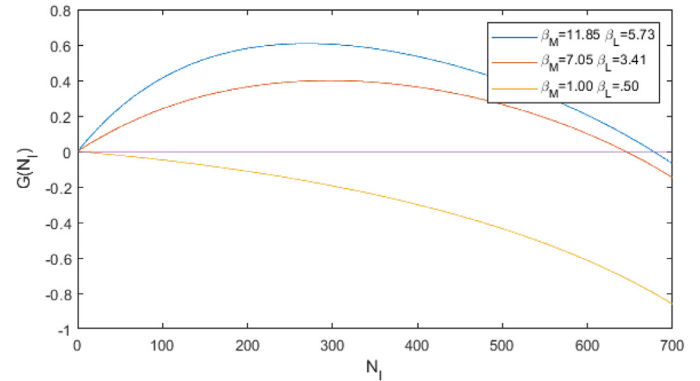


Fig. 3. An endemic equilibrium of the model is a root of the function  $G$ .

given in Table 3;  $\mathcal{R}_C > 1$  (and thus an endemic equilibrium exists) for the first two curves, but not for the lower curve.

Local stability analysis for the endemic equilibrium via the Jacobian matrix shows the endemic equilibrium is locally asymptotically stable when it exists; see Appendix A.5 for details.

## 4. Numerical results

### 4.1. Parameter estimation

Estimated values for model parameters are given in Table 3. Where possible, they were taken from prior studies; in other cases, key parameters (infection rates  $\beta_*$  and the vaccination rate  $\psi$ ) were varied in numerical analysis, as detailed below. Most of these parameters are given as rates in units of 1/year, often converted from 1/day as found in literature.

The total mouse population of 50 and total nymph population of 1000 were estimated using data on mice and tick populations in fragmented forest areas, relating woodland size to population density. We focused on plot sizes of 1.1 hectares to match the study that gave us our proportion of vaccine effectiveness (Schwendinger et al., 2013). Though the data varied, we chose populations that had biological significance and would allow us to simulate our model. Values  $\Delta_M$  and  $\Delta_T$  were calculated from the population death rates and sizes, using the equilibrium solutions for the total mouse and tick populations as found in Appendix A.2.

Values for the tick death rates  $\alpha_1$ ,  $\alpha_2$ , and  $\alpha_3$  were derived from survival proportions between each stage of the tick life cycle; exact calculations are in Appendix A.6.

The three sets of  $\beta$  values in units of 1/year,  $\beta_M = 0.68$ ,  $0.86$ , and  $1.47$ ,  $\beta_L = 3.41$ ,  $4.29$ , and  $5.73$ , and  $\beta_M = 7.05$ ,  $8.87$ , and  $11.85$ , were estimated to signify very low, moderate, and high transmission rates, each respectively corresponding to approximately 20%, 35% and 50% of nymphs infected at equilibrium. Since biting rates between ticks and mice are dependent on abiotic factors and proportions of other nymph hosts that are not present in our model, we wanted to use  $\beta$  values that would provide information on a wide range of biologically feasible scenarios. All calculations for parameter values are explained further in Appendix A.6.

### 4.2. Numerical analysis

Simulations were implemented using MATLAB. Baseline results with parameter values as given in Table 3, intermediate infection rates as given above, and vaccination rate  $\psi = 10$ /year, showed populations reaching equilibrium within 6 years, and vaccination driving a high endemic prevalence in ticks to a low one (see Fig. 4).

Examining endemic prevalence levels as functions of the infectious contact rates (Fig. 5) revealed a low, saturating asymptotic

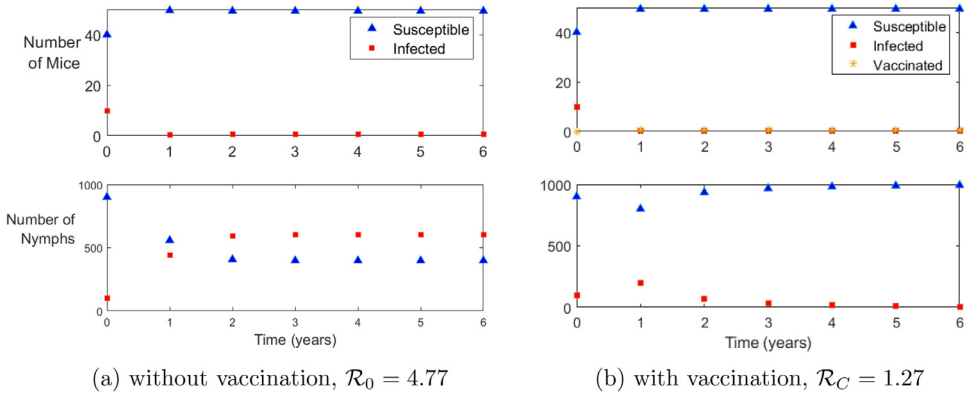


**Fig. 4.** Mouse (upper graphs) and nymph (lower graphs) populations with and without vaccination at  $\beta_N=0.86/\text{year}$ ,  $\beta_L=4.29/\text{year}$ ,  $\beta_M=8.87/\text{year}$ .

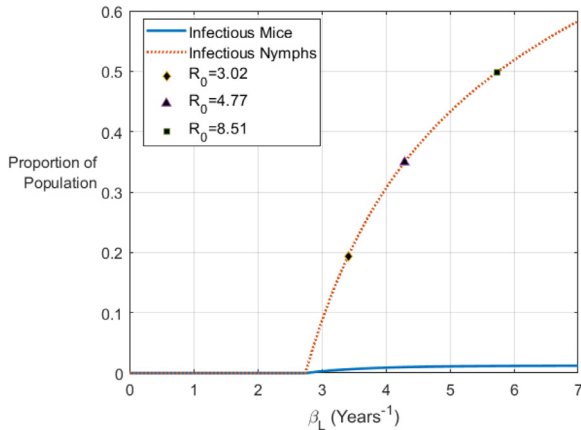


**Fig. 5.** Asymptotic fixed points for infected mice and nymph proportions of population as  $\beta_L$  varies,  $\psi = 0$ ,  $\mathcal{R}_0 \in [0, 12.68]$ .

value of approximately 1.2% for endemic prevalence in mice as infection rates increase (in the absence of vaccination,  $\psi = 0$ ).<sup>1</sup> This can be explained by the ordering of events in our model, specifically observing that three-fourths of mouse recruitment takes place at the end of the year. Since all mice are born susceptible, these mice are counted as susceptible at our sampling time in the next spring. Even if 100% of mice were to be infected after the nymph biting period, those mice must survive fall, winter, and most of spring to affect the next cycle, which gives biological justification to the trend in Fig. 5 explained above. Due to the short life span of the mice, only a very low proportion of them actually make it to the next spring, so biologically there should always be a minimum number of susceptible mice in the spring.

Another important finding of this analysis is that endemic prevalence in mice reaches this asymptotic limit at a point ( $\beta_L = 4/\text{yr}$  in Fig. 5) where the proportion of infected nymphs is still approximately 30%. This means that the spring population of mice is not a good predictor of the proportion of infected nymphs that year as the percent of nymphs infected could vary from 30% to 100% with very little measurable change in mouse infection prevalence. Additionally, the infected mouse population is so small for

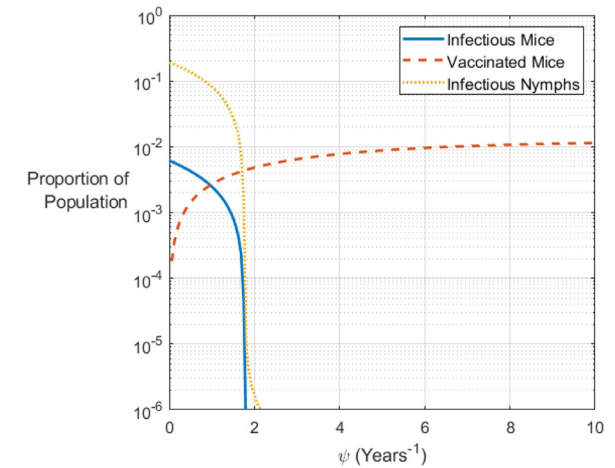


**Fig. 6.** Equilibrium population proportions at low contact rates as  $\psi$  varies with  $\beta_N = 0.68/\text{year}$ ,  $\beta_L = 3.41/\text{year}$ ,  $\beta_M = 7.05/\text{year}$ ,  $\mathcal{R}_C \in [0.18, 3.02]$ .

any infectious contact rates that any field estimation would be very difficult. In short, while the exact maximum proportion of infected mice will vary between geographical regions and mice habitats, the proportion of infected mice measured in the spring is not a good predictor for Lyme disease risk that year.

To analyze the effect of vaccination on the transmission cycle, we graph endemic equilibria with respect to varying vaccination rates,  $\psi$ , at the low (Fig. 6), medium (Fig. 7), and high (Fig. 8) test values for contact rates between mice and ticks discussed in our parameter estimation. These plots show that the number of infected ticks can be reduced to less than one (less than  $10^{-3}$  proportion infected since the nymphal population size is 1000) at vaccination rates of approximately 2/year, 4/year, and 6/year<sup>2</sup> for the low, medium, and high sets of infectious contact rate values respectively. This shows an approximately linear relationship between endemic prevalence in ticks without vaccination and the vaccination rate required to control the epidemic. If equilibrium infection prevalence increases by 15% then the vaccination rate required to eliminate the pathogen is an additional 2/year. For example, the low set of contact rates which correspond to approximately 20% of nymphs infected require a vaccination rate of 2/year to be reduced to less than one infected tick (Fig. 6). The medium contact rates which correspond to approximately 35% infected require a vaccination rate of 4/year to be reduced to less than one in-

<sup>1</sup> We vary infectious contact rates by keeping a constant ratio between  $\beta_N$ ,  $\beta_L$ , and  $\beta_M$ . There is a set ratio between the mouse and the nymphal contact rate because both depend on the rate at which ticks bite mice. To convert the tick biting rate to the mouse biting rate, we multiplied by the proportion of nymphs to mice. We then set  $\beta_N$  to vary from 0 to 1.2/yr and then tested varying ratios between  $\beta_N$  and  $\beta_L$  until we found sets of contact rates that corresponded to percent nymphs infected at equilibrium that matched biological expectations (Richer et al., 2014).

<sup>2</sup> A note on interpretation: A vaccination rate of  $\psi = 6/\text{year}$  means it takes one mouse an average of 1/6 of a year to encounter a bait box.

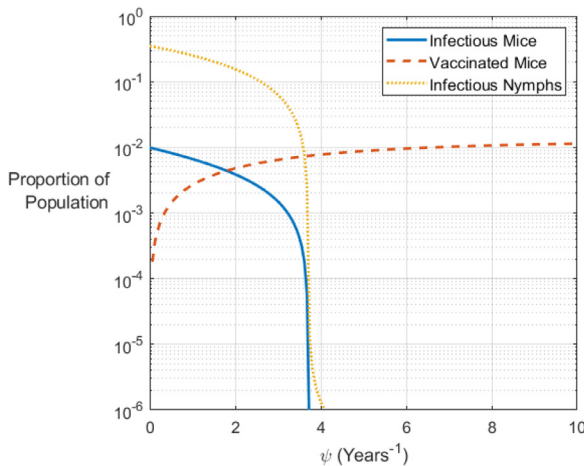


**Fig. 7.** Equilibrium population proportions at medium contact rates as  $\psi$  varies with  $\beta_N = 0.86/\text{year}$ ,  $\beta_L = 4.29/\text{year}$ ,  $\beta_M = 8.87/\text{year}$ ,  $\mathcal{R}_C \in [0.28, 4.77]$ .

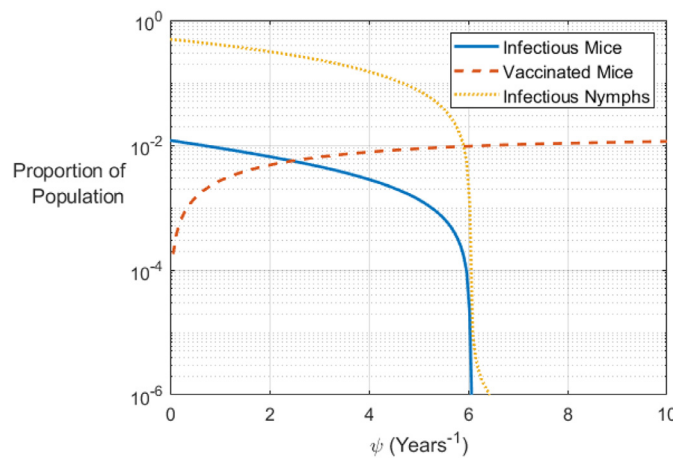


**Fig. 8.** Equilibrium population proportions at high contact rates as  $\psi$  varies with  $\beta_N = 1.47/\text{year}$ ,  $\beta_L = 5.73/\text{year}$ ,  $\beta_M = 11.85/\text{year}$ ,  $\mathcal{R}_C \in [0.48, 8.51]$ .

fected tick (Fig. 7). A similar change is seen again from the medium contact rates to the high contact rates, corresponding to 50% of nymphs infected, as they require a vaccination rate of 6 per year to be reduced to less than one infected nymph (Fig. 8). This can be a guide to those seeking to introduce vaccination across a variety of areas who may not have the aid of computational tools to recalculate vaccination rates for each area.

We note that the values of the vaccination rate  $\psi$  required to reduce the control reproduction number  $\mathcal{R}_C$  to less than 1 are significantly greater than the vaccination rates required to reduce the number of infected ticks to less than 1. For small  $\beta$  values, this is at  $\psi = 4.58/\text{year}$ , for medium  $\beta$  values, it is at  $\psi = 6.55/\text{year}$ , and at large  $\beta$  values, this is at  $\psi = 11.04/\text{year}$ . The practical difference between these two thresholds lies in the scale of the population being modeled: as the total population size increases, the minimum detectable endemic prevalence approaches 0 and the two thresholds converge. We remind the reader that our choice of scale here reflects the model's implicit assumption that the populations mix homogeneously.

Since equilibria may take many years to reach, we also mapped the effect of vaccination on the proportion of infected nymphs after two, five, and ten years in Fig. 9. These results showed that, not only can vaccinating mice significantly reduce the endemic prevalence, it can do so within short time periods. Vaccination was effective at reducing the number of infected nymphs to zero for all

infectious contact rates within the range of vaccination rates sampled. As the figure indicates, equilibrium proportions of infected ticks above 20% were reached quickly (within two years) but the time required to reach lower equilibrium prevalences in ticks depended strongly on vaccination rates. This means that reaching equilibrium prevalences lower than 20% typically takes more than two years (but can be accelerated by increasing vaccination): if the proportion of infected ticks is above 20%, individuals using vaccines to reduce the number of infected ticks should expect to see the same results every year after two years; however, for lower proportions, they should see a lower number of infected ticks each year if continuing to vaccinate at the same rate.

#### 4.3. Risk and cost analysis

Through risk and cost analysis we can understand the effectiveness of mouse vaccination at reducing human cases of Lyme disease. We have determined that vaccines can significantly reduce the number of infected nymphal ticks in an area; thus we also compare the cost of vaccination with reductions of human risk to determine if the intervention is cost saving. In order to predict the change in the risk of human Lyme disease cases, we construct the following function for the yearly number of new human cases,  $I(t)$ , also known as the incidence rate:

$$I(t) = \rho \cdot \gamma \cdot H_S \cdot \frac{N_I(t)}{N},$$

where  $\gamma$  is the biting rate of tick nymph per human per year,  $H_S$  is the number of humans at risk,  $\rho$  is the probability of infection for humans after a bite from an infected nymph, and  $N_I(t)/N$  is the current infection prevalence in nymphs (dependent on  $\psi$  and  $\beta$  values). Although adult ticks also bite humans, we do not include these contacts in our model because this is minimal in terms of transmitting infection to humans; due to the large size of these ticks, most are detected and removed before the necessary time to transmit the infection (Caraco et al., 2002; Ostfeld et al., 1995). We take the value of  $\rho$  to be 0.031, obtained by taking an average from a range of values in our source (Magid et al., 1992). We found  $\gamma$  to be valued at 0.005/day, or equivalently 0.913/year,<sup>3</sup> from another model but decided to vary this value since it was unclear how this  $\gamma$  had been calculated (Wang and Zhao, 2017).

More precisely,  $H_S$  is the number of people who spend their tick exposure time in that tick-infected region. There are three components to  $H_S$ . First is the yearly number of unique people that move through an area. Second is the average percentage of those people's tick exposure time spent in the vaccination area. Third is the percentage of that area covered by 1 hectare. For example, 1000 unique people may walk on a suburban trail in a year. Since this a neighborhood trail, most of those people likely walk dogs or spend time with their children regularly there, so the average person may spend 80% of their total time exposed to ticks on that trail. Finally, that trail may be a kilometer long, so if mice are vaccinated for 50 m on either side of the trail, the total vaccination area would be 5 hectares; thus a single hectare of vaccination would only cover 20% of the total trail risk. This gives us our first estimated  $H_S$  value of  $1000 * 0.8 * 0.2 = 160$ . The other two estimated values follow similarly. One accounts for a similar trail, but less populated, and the other represents a public park. Table 4 compares these three scenarios.

To analyze the cost of Lyme disease treatment, we examine the relationship between total cost of implementing mouse vaccination and average cost for Lyme disease treatment per infected person. We assume a linear relationship between the vaccination rate  $\psi$

<sup>3</sup>  $0.005 * 365 = 1.825/\text{year}$ . Nymphs are active for only half the year, and  $1.825/2 \approx 0.913$ .

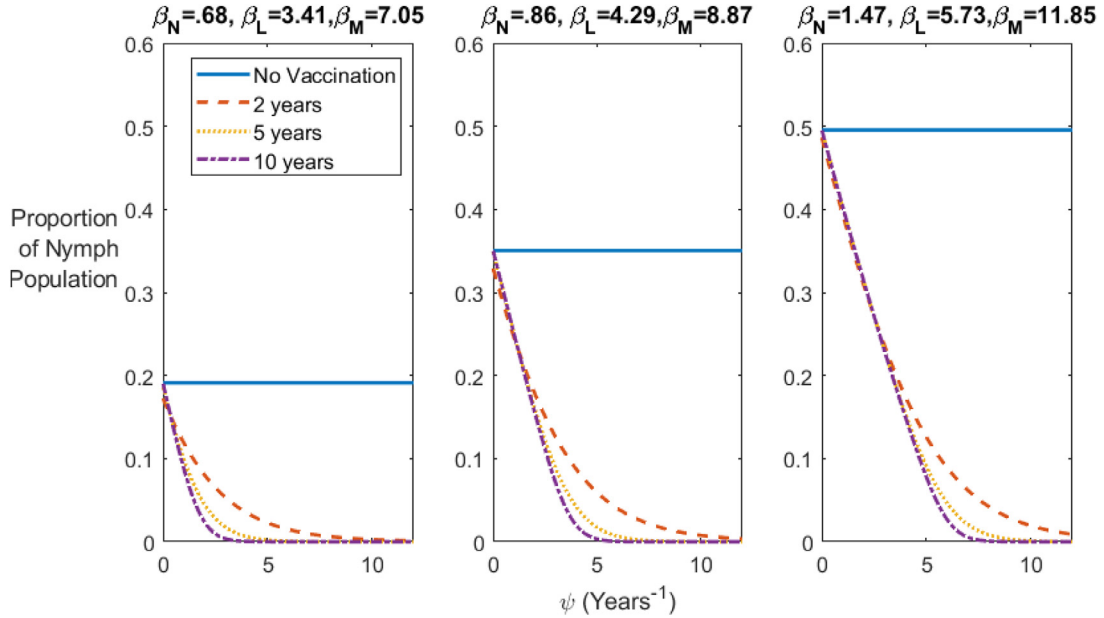


**Fig. 9.** Vaccine effect on nymphs compared to years of use for low, medium, and high contact rates,  $\mathcal{R}_C \in [0.18, 3.02]$ ,  $\mathcal{R}_C \in [0.28, 4.77]$ , and  $\mathcal{R}_C \in [0.48, 8.51]$  ( $\beta$  values in 1/yr). In each case the corresponding endemic equilibrium without vaccination was used for initial conditions.

**Table 4**  
Scenarios for estimation of  $H_S$  values.

$H_S$ value	80	160	750
Geographical area	Trail	Trail	Park
Number of people	500	1000	5000
Proportion of time spent	80%	80%	30%
Proportion of area covered	20%	20%	50%

and the increase in cost per increase in vaccination rate,  $x$ . Since white-footed mice are territorial, it is possible that a particular nest of mice are the only ones feeding from a particular bait box (Aguilar, 2018). Thus, the same number of mice would access each box regardless of the number of boxes until all mice are vaccinated, making this assumption biologically feasible. This achieves the following cost function,

$$C_{total} = x \cdot \psi + I \cdot \theta,$$

where  $\theta$  is the average cost of Lyme disease treatment per infection, calculated to be \$3537.70 per person within the first 12 months following diagnosis with Lyme disease based on studies of health care costs of Lyme disease (Adrion et al., 2015), as shown in Appendix A.6. Using data from a field study of vaccines targeting white-footed mice, we estimated  $x$  to be \$329.29 per unit increase in  $\psi$  (Interlandi, 2018; Richer et al., 2014), as shown in Appendix A.6. Since we are assessing cost over a 10 year period we calculate cost taking into account inflation and use the September 2018–September 2019 consumer price index (CPI) change of 1.7% as the approximate inflation rate (U. S. Bureau of Labor Statistics, 2019). Since we calculate cost discretely in our model, we assume costs are accumulated at the end of each year assessed. This means that since we assessing cost in current year dollars, the cost accumulated in the first year for example would be the base cost  $C_{t=1}^*$  times  $R^{10-1} = R^9$ , where  $R = 1.017$  is our inflation rate, to get  $C_{t=1} = C_{t=1}^* * R^9 = 1.164C_{t=1}^*$ . Thus the total cost will be given as

$$C_{t=i} = \left( x \cdot \psi + \theta \cdot \rho \cdot \gamma \cdot H_S \frac{N_t}{N} \right) * R^{10-i}. \quad (7)$$

For a summary of parameter definitions and values for the cost function see Table 5.

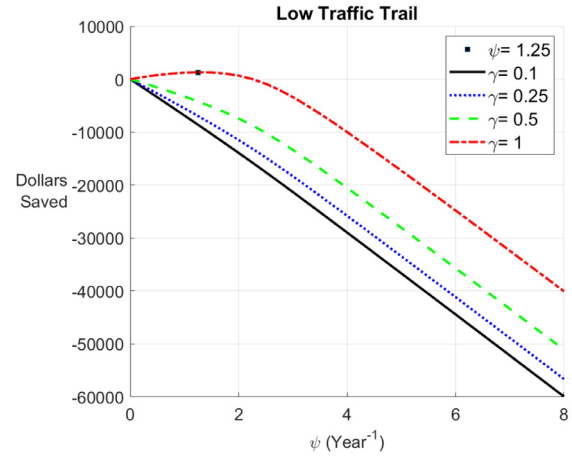


**Fig. 10.** Dollars saved after 10 years of vaccination on a low traffic trail for varying nymphal biting rates,  $H_S = 80$ , medium contact rates. Negative dollars saved means more money was spent than saved. Only at the highest tick feeding rate was vaccination cost saving.

Since  $N_t$  is a decreasing function of  $\psi$ , we have an optimization problem to adjust vaccination rate to maximize cost savings (relative to no vaccination) for a human population infected with Lyme disease and mouse vaccination intervention after ten years across varying values of  $\gamma$ . Figs. 10–12 represent susceptible populations of 80, 160, and 750 humans, respectively. In all of these plots we observe a similar trend in that the higher the biting rate  $\gamma$ , the more money saved. However, only for a human population size of 1000 does vaccination become cost saving for every  $\gamma$  value. In each case there is a cost-optimal value for  $\psi$ . The greater the human population, the greater this optimal vaccination rate. The cost savings also scale up for larger human populations. In the parks, with the highest number of susceptible humans, vaccination saved up to approximately \$170,000 in the first ten years, whereas significantly less money is saved from vaccinating on trails. We note that even if minimal money is saved from vaccinations, the inter-

**Table 5**

Parameters, with values, for risk and cost equations.

Param.	Definition	Unit	Value	Source
$x$	Increase in cost per increase in vaccination rate	dollars	\$329.29	(Richer et al., 2014)
$\psi$	Contact between mice and vaccines	1/year	varied	–
$\theta$	Average cost of Lyme disease treatment	dollars/infection	\$3537.70	(Adrion et al., 2015)
$\rho$	Probability of infection for humans after nymph bite	infections/bites	0.031	(Magid et al., 1992)
$\gamma$	Biting rate of tick nymph per human per year	bites/(human · yr)	varied	–
$H_S$	Susceptible humans	people	varied	–
$R$	Inflation Rate	–	1.017	(U. S. Bureau of Labor Statistics, 2019)

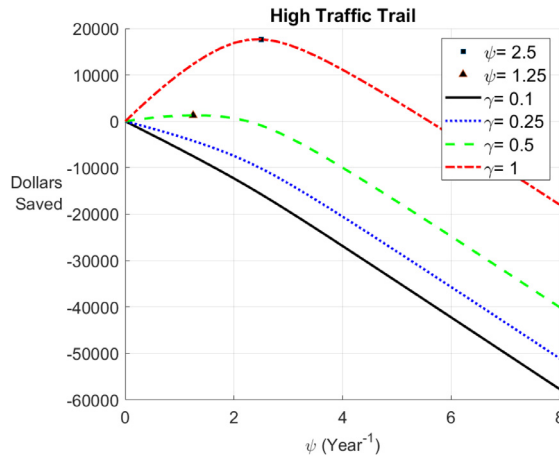


**Fig. 11.** Dollars saved after 10 years of vaccination on a high traffic trail for varying nymphal biting rates,  $H_S = 160$ , medium contact rates. Negative dollars saved means more money was spent than saved. Vaccination was cost saving at moderate to high tick feeding rates.

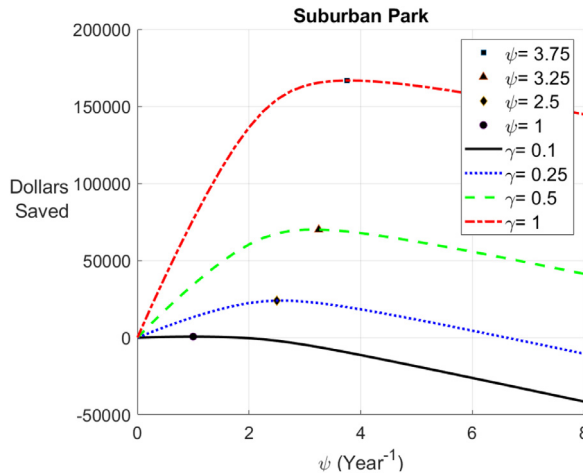


**Fig. 12.** Dollars saved after 10 years of vaccination in a suburban park for varying nymphal biting rates,  $H_S = 750$ , medium contact rates. Negative dollars saved means more money was spent than saved. Vaccination was extremely cost saving.

vention will still reduce cases of Lyme disease, improving public health in the local community.

This analysis reflects that vaccines can be a cost saving method when compared to treatment for Lyme disease but likely only in areas where mice come into frequent contact with bait boxes, especially in areas with a high level of human traffic.

## 5. Discussion

This study used a coupled mouse ( $M_S$ ,  $M_I$ ,  $M_V$ ) and nymphal tick ( $N_S$ ,  $N_I$ ) model to determine whether vaccinating mouse populations in fragmented forests could reduce the number of Lyme-

infected ticks there. This model captures both the seasonal dynamics of the mouse-tick interactions and the effects of vaccination on the persistence of the infection. These characteristics are important because an accurate estimate of infection prevalence within the nymphal stage relates directly to the expected number of human cases in an area and the cost saving potential of vaccines.

Analysis showed that vaccination can eliminate local *B. burgdorferi* transmission between mice and ticks at achievable rates and duration of vaccination. Additionally, we found that the vaccination rates required to reduce infection prevalence in ticks to 20% achieved the reduction within two years, whereas the time required to reach lower prevalences was sensitive to vaccination rates. Thus infected tick prevalence can be reduced to 20% within the first two years, but reduction to trace levels would likely take longer.

Furthermore, the cost analysis shows that vaccine intervention is cost saving in specific targeted areas where mice are primary reservoirs if there is significant human presence in the area, especially if ticks bite humans frequently there. We believe this could be a particularly practical measure in fragmented forests near human settlements like parks or wooded areas in and around suburban developments. These environments often have very high infection prevalence among nymphal ticks, low mammal diversity, and high levels of human activity.

In future research, this model could be adapted to include influence of other control factors. Some promising methods include chemical or fungal pesticides to cull tick populations, or increasing mammalian biodiversity to allow for predation or for competition with less competent reservoirs of small mammal hosts. Modeling the pesticide methods could include adding classes of mice that are protected by pesticide applied directly to their fur through bait boxes similar to the ones that deliver the vaccine. Increased biodiversity might include predator-prey or competition dynamics with different species of host having different transmission rates. A more detailed cost analysis would also be possible. Incorporating the effects of tick diapause could improve model accuracy. Lyme disease is a significant public health problem, and a variety of mathematical models could offer solutions without the need for expensive field tests.

## Declaration of Competing Interest

None.

## CRedit authorship contribution statement

**Daniel Carrera-Pineyro:** Conceptualization, Methodology, Software, Formal analysis, Writing - original draft. **Harley Hanes:** Conceptualization, Methodology, Software, Formal analysis, Writing - original draft, Writing - review & editing. **Adam Litzler:** Conceptualization, Methodology, Software, Formal analysis, Writing - original draft. **Andrea McCormack:** Conceptualization, Methodology, Software, Formal analysis, Writing - original draft. **Josean Velazquez-Molina:** Supervision. **Anuj Mubayi:** Supervision, Fund-

ing acquisition. **Karen Ríos-Soto:** Supervision. **Christopher Kribs:** Supervision, Formal analysis, Writing - review & editing.

## Acknowledgments

The authors thank the directors and staff of the Mathematical and Theoretical Biology Institute (MTBI) at Arizona State University, where this research was performed, particularly founding director Dr. Carlos Castillo-Chavez, Ms. Rebecca Perlin, and Ms. Sabrina Avila. Through MTBI, this project was partially supported by grants from the **National Science Foundation** (NSF Grant **MPS-DMS-1263374** and NSF Grant **DMS-1757968**), the **National Security Agency** (NSA Grant **H98230-J8-1-0005**), the Alfred P. Sloan Foundation, the Office of the President of ASU, and the Office of the Provost of ASU.

## Appendix A

### A1. Single-event transition equations

The following table describes the effect of each possible model event on the relevant populations. Here  $c$  is the proportion of the year for which the particular process takes place. This is not constant for a given compartment transition and depends on the order of events and transitions being divided into multiple events. Also,  $M(t) = M_I(t) + M_V(t) + M_S(t)$  is the total mouse population at time  $t$ , while  $N(t) = N_S(t) + N_I(t)$  counts all tick nymphs at time  $t$ .

Mouse events		
Event	Flow	Term in equation
Mice are born	$\rightarrow M_S$	$M_S(t + \frac{i+1}{k}) = c\Lambda_M + M_S(t + \frac{i}{k})$
Mice are vaccinated	$M_S \rightarrow M_V$	$M_S(t + \frac{i+1}{k}) = M_S(t + \frac{i}{k})e^{-c\psi\omega}$
Mice die	$M_S \rightarrow M_I$	$M_V(t + \frac{i+1}{k}) = M_V(t + \frac{i}{k}) + M_S(t + \frac{i}{k})(1 - e^{-c\psi\omega})$
	$M_I \rightarrow M_I$	$M_S(t + \frac{i+1}{k}) = M_S(t + \frac{i}{k})e^{-c\mu}$
	$M_I \rightarrow M_I$	$M_I(t + \frac{i+1}{k}) = M_I(t + \frac{i}{k})e^{-c\mu}$
	$M_V \rightarrow M_V$	$M_V(t + \frac{i+1}{k}) = M_V(t + \frac{i}{k})e^{-c\mu}$
Mice are infected	$M_S \rightarrow M_I$	$M_S(t + \frac{i+1}{k}) = M_S(t + \frac{i}{k})e^{-c\beta_M \frac{N_I(t + \frac{i}{k})}{N(t + \frac{i}{k})}}$
		$M_I(t + \frac{i+1}{k}) = M_I(t + \frac{i}{k}) + M_S(t + \frac{i}{k}) \left(1 - e^{-c\beta_M \frac{N_I(t + \frac{i}{k})}{N(t + \frac{i}{k})}}\right)$
Tick events		
Event	Flow	Term in equation
Ticks die	$L_S \rightarrow L_S$	$L_S(t + \frac{i+1}{k}) = L_S(t + \frac{i}{k})e^{-c\alpha}$
	$N_S \rightarrow N_S$	$N_S(t + \frac{i+1}{k}) = N_S(t + \frac{i}{k})e^{-c\alpha}$
	$N_I \rightarrow N_I$	$N_I(t + \frac{i+1}{k}) = N_I(t + \frac{i}{k})e^{-c\alpha}$
	$A_S \rightarrow A_S$	$A_S(t + \frac{i+1}{k}) = A_S(t + \frac{i}{k})e^{-c\alpha}$
	$A_I \rightarrow A_I$	$A_I(t + \frac{i+1}{k}) = A_I(t + \frac{i}{k})e^{-c\alpha}$
Larvae feed	$L_S \rightarrow N_I$	$N_I(t + \frac{i+1}{k}) = L_S(t + \frac{i}{k})e^{-c\beta_L \frac{M_I(t + \frac{i}{k})}{M(t + \frac{i}{k})}}$
	$L_S \rightarrow N_S$	$N_S(t + \frac{i+1}{k}) = L_S(t + \frac{i}{k}) \left(1 - e^{-c\beta_L \frac{M_I(t + \frac{i}{k})}{M(t + \frac{i}{k})}}\right)$
Nymphs feed	$N_I \rightarrow A_I$	$A_I(t + \frac{i+1}{k}) = N_I(t + \frac{i}{k})$
	$N_S \rightarrow A_I$	$A_I(t + \frac{i+1}{k}) = N_S(t + \frac{i}{k})e^{-c\beta_N \frac{M_I(t + \frac{i}{k})}{M(t + \frac{i}{k})}}$
	$N_S \rightarrow A_S$	$A_S(t + \frac{i+1}{k}) = N_S(t + \frac{i}{k}) \left(1 - e^{-c\beta_N \frac{M_I(t + \frac{i}{k})}{M(t + \frac{i}{k})}}\right)$
Larvae hatch	$\rightarrow L_S$	$L_S(t + \frac{i+1}{k}) = L_S(t + \frac{i}{k}) + c\Lambda_T$

### A2. Model derivation

Again let  $M(t) = M_S(t) + M_I(t) + M_V(t)$  and  $N(t) = N_S(t) + N_I(t)$ .

#### 1. Mice are vaccinated

$$M_S\left(t + \frac{1}{11}\right) = M_S(t)e^{-\frac{\psi\omega}{4}}$$

$$M_V\left(t + \frac{1}{11}\right) = M_V(t) + M_S(t)(1 - e^{-\frac{\psi\omega}{4}})$$

#### 2. Nymphs infect mice

$$\begin{aligned} M_S\left(t + \frac{2}{11}\right) &= M_S\left(t + \frac{1}{11}\right)e^{-\frac{\beta_M}{2} \frac{N_I(t)}{N(t)}} \\ &= M_S(t)e^{-\frac{\psi\omega}{4}}e^{-\frac{\beta_M}{2} \frac{N_I(t)}{N(t)}} \\ M_I\left(t + \frac{2}{11}\right) &= M_I\left(t + \frac{1}{11}\right) + M_S\left(t + \frac{1}{11}\right)\left(1 - e^{-\frac{\beta_M}{2} \frac{N_I(t)}{N(t)}}\right) \\ &= M_I(t) + M_S(t)e^{-\frac{\psi\omega}{4}}\left(1 - e^{-\frac{\beta_M}{2} \frac{N_I(t)}{N(t)}}\right) \end{aligned}$$

#### 3. Susceptible and infected nymphs feed on mice and become infected adults

$$\begin{aligned} A_I\left(t + \frac{3}{11}\right) &= N_I\left(t + \frac{2}{11}\right) + N_S\left(t + \frac{2}{11}\right)\left(1 - e^{-\frac{\beta_N}{2} \frac{M_I(t + \frac{2}{11})}{M(t + \frac{2}{11})}}\right) \\ &= N_I(t) + N_S(t) \\ &\quad \left(1 - \exp\left[-\frac{\beta_N}{2} \frac{M_I(t) + M_S(t)e^{-\frac{\psi\omega}{4}}\left(1 - e^{-\frac{\beta_M}{2} \frac{N_I(t)}{N(t)}}\right)}{M(t)}\right]\right) \end{aligned}$$

#### Susceptible nymphs become susceptible adults

$$\begin{aligned} A_S\left(t + \frac{3}{11}\right) &= N_S\left(t + \frac{2}{11}\right)\left(e^{-\frac{\beta_N}{2} \frac{M_I(t + \frac{2}{11})}{M(t + \frac{2}{11})}}\right) \\ &= N_S(t) \exp\left(-\frac{\beta_N}{2} \frac{M_I(t) + M_S(t)e^{-\frac{\psi\omega}{4}}\left(1 - e^{-\frac{\beta_M}{2} \frac{N_I(t)}{N(t)}}\right)}{M(t)}\right) \end{aligned}$$

#### 4. Mice die

$$\begin{aligned} M_S\left(t + \frac{4}{11}\right) &= M_S\left(t + \frac{3}{11}\right)e^{-\frac{\mu}{4}} \\ &= M_S(t)e^{-\frac{\mu}{4}}e^{-\frac{\psi\omega}{4}}e^{-\frac{\beta_M}{2} \frac{N_I(t)}{N(t)}} \\ M_I\left(t + \frac{4}{11}\right) &= M_I\left(t + \frac{3}{11}\right)e^{-\frac{\mu}{4}} \\ &= M_I(t)e^{-\frac{\mu}{4}} + M_S(t)e^{-\frac{\mu}{4}}e^{-\frac{\psi\omega}{4}}\left(1 - e^{-\frac{\beta_M}{2} \frac{N_I(t)}{N(t)}}\right) \\ M_V\left(t + \frac{4}{11}\right) &= M_V\left(t + \frac{3}{11}\right)e^{-\frac{\mu}{4}} \\ &= M_V(t)e^{-\frac{\mu}{4}} + M_S(t)e^{-\frac{\mu}{4}}\left(1 - e^{-\frac{\psi\omega}{4}}\right) \end{aligned}$$

#### 5. Mice are born

$$\begin{aligned} M_S\left(t + \frac{5}{11}\right) &= M_S\left(t + \frac{4}{11}\right) + \frac{\Lambda_M}{4} \\ &= M_S(t)e^{-\frac{\mu}{4}}e^{-\frac{\psi\omega}{4}}e^{-\frac{\beta_M}{2} \frac{N_I(t)}{N(t)}} + \frac{\Lambda_M}{4} \end{aligned}$$

#### 6. Larvae hatch

$$L_S\left(t + \frac{6}{11}\right) = L_S\left(t + \frac{5}{11}\right) + \Lambda_T = \Lambda_T$$

#### 7. Larvae die

$$L_S\left(t + \frac{7}{11}\right) = L_S\left(t + \frac{6}{11}\right)e^{-\frac{\alpha_1}{4}} = e^{-\frac{\alpha_1}{4}}\Lambda_T$$

#### 8. Larvae feed, possibly get infected, and transition to nymphs

$$\begin{aligned} N_S\left(t + \frac{8}{11}\right) &= L_S\left(t + \frac{7}{11}\right)\left(e^{-\frac{\beta_L}{2} \frac{M_I(t + \frac{7}{11})}{M(t + \frac{7}{11})}}\right) \\ &= \Lambda_T e^{-\frac{\alpha_1}{4}} \exp\left(-\frac{\beta_L}{4} \frac{M_I(t)e^{-\frac{\mu}{4}} + M_S(t)e^{-\frac{\mu}{4}}e^{-\frac{\psi\omega}{4}}\left(1 - e^{-\frac{\beta_M}{2} \frac{N_I(t)}{N(t)}}\right)}{e^{-\frac{\mu}{4}}M(t) + \frac{\Lambda_M}{4}}\right) \end{aligned}$$

$$N_I\left(t + \frac{8}{11}\right) = L_S\left(t + \frac{7}{11}\right) \left(1 - e^{-\frac{\beta_I}{4} \frac{M_I(t + \frac{7}{11})}{M(t + \frac{7}{11})}}\right)$$

$$= \Lambda_T e^{-\frac{\alpha_1}{4}}$$

$$\times \left(1 - \exp \left[ -\frac{\beta_L}{4} \frac{M_I(t)e^{-\frac{\mu}{4}} + M_S(t)e^{-\frac{\mu}{4}} e^{-\frac{\psi\omega}{4}} \left(1 - e^{-\frac{\beta_M}{2} \frac{N_I(t)}{N(t)}}\right)}{e^{-\frac{\mu}{4}} M(t) + \frac{\Lambda_M}{4}} \right] \right)$$

9. Nymphs die

$$N_S\left(t + \frac{9}{11}\right) = N_S\left(t + \frac{8}{11}\right) e^{-\frac{3\alpha_2}{4}}$$

$$= \Lambda_T e^{-\frac{(\alpha_1+3\alpha_2)}{4}} \exp$$

$$\times \left( -\frac{\beta_L}{4} \frac{M_I(t)e^{-\frac{\mu}{4}} + M_S(t)e^{-\frac{\mu}{4}} e^{-\frac{\psi\omega}{4}} \left(1 - e^{-\frac{\beta_M}{2} \frac{N_I(t)}{N(t)}}\right)}{e^{-\frac{\mu}{4}} M(t) + \frac{\Lambda_M}{4}} \right)$$

$$N_I\left(t + \frac{9}{11}\right) = N_I\left(t + \frac{8}{11}\right) e^{-\frac{3\alpha_2}{4}}$$

$$= \Lambda_T e^{-\frac{(\alpha_1+3\alpha_2)}{4}} \times \left( 1 - \exp \left[ -\frac{\beta_L}{4} \frac{M_I(t)e^{-\frac{\mu}{4}} + M_S(t)e^{-\frac{\mu}{4}} e^{-\frac{\psi\omega}{4}} \left(1 - e^{-\frac{\beta_M}{2} \frac{N_I(t)}{N(t)}}\right)}{e^{-\frac{\mu}{4}} M(t) + \frac{\Lambda_M}{4}} \right] \right)$$

10. Mice die

$$M_S\left(t + \frac{10}{11}\right) = M_S\left(t + \frac{9}{11}\right) e^{-\frac{3\mu}{4}}$$

$$= M_S(t)e^{-\mu} e^{-\frac{\psi\omega}{4}} e^{-\frac{\beta_M}{2} \frac{N_I(t)}{N(t)}} + \frac{\Lambda_M}{4} e^{-\frac{3\mu}{4}}$$

$$M_I\left(t + \frac{10}{11}\right) = M_I(t)e^{-\mu} + M_S(t)e^{-\mu} e^{-\frac{\psi\omega}{4}} \left(1 - e^{-\frac{\beta_M}{2} \frac{N_I(t)}{N(t)}}\right)$$

$$M_V\left(t + \frac{10}{11}\right) = M_V(t)e^{-\mu} + M_S(t)e^{-\mu} \left(1 - e^{-\frac{\psi\omega}{4}}\right)$$

11. Mice are born

$$M_S(t+1) = M_S(t)e^{-\mu} e^{-\frac{\psi\omega}{4}} e^{-\frac{\beta_M}{2} \frac{N_I(t)}{N(t)}} + \frac{\Lambda_M}{4} e^{-\frac{3\mu}{4}} + \frac{3\Lambda_M}{4}$$

$$= M_S(t)e^{-\mu} e^{-\frac{\psi\omega}{4}} e^{-\frac{\beta_M}{2} \frac{N_I(t)}{N(t)}} + \frac{\Lambda_M}{4} \left(e^{-\frac{3\mu}{4}} + 3\right)$$

12. Final equations

$$N_I(t+1) = \Lambda_T e^{-\frac{(\alpha_1+3\alpha_2)}{4}}$$

$$\left(1 - \exp \left[ -\frac{\beta_L}{4} \frac{M_I(t)e^{-\frac{\mu}{4}} + M_S(t)e^{-\frac{\mu}{4}} e^{-\frac{\psi\omega}{4}} \left(1 - e^{-\frac{\beta_M}{2} \frac{N_I(t)}{N(t)}}\right)}{e^{-\frac{\mu}{4}} M(t) + \frac{\Lambda_M}{4}} \right] \right)$$

$$N_S(t+1) = \Lambda_T e^{-\frac{(\alpha_1+3\alpha_2)}{4}}$$

$$\exp \left( -\frac{\beta_L}{4} \frac{M_I(t)e^{-\frac{\mu}{4}} + M_S(t)e^{-\frac{\mu}{4}} e^{-\frac{\psi\omega}{4}} \left(1 - e^{-\frac{\beta_M}{2} \frac{N_I(t)}{N(t)}}\right)}{e^{-\frac{\mu}{4}} M(t) + \frac{\Lambda_M}{4}} \right)$$

$$M_S(t+1) = M_S(t)e^{-\mu} e^{-\frac{\psi\omega}{4}} e^{-\frac{\beta_M}{2} \frac{N_I(t)}{N(t)}} + \frac{\Lambda_M}{4} \left(e^{-\frac{3\mu}{4}} + 3\right)$$

$$M_I(t+1) = M_I(t)e^{-\mu} + M_S(t)e^{-\mu} e^{-\frac{\psi\omega}{4}} \left(1 - e^{-\frac{\beta_M}{2} \frac{N_I(t)}{N(t)}}\right)$$

$$M_V(t+1) = M_V(t)e^{-\mu} + M_S(t)e^{-\mu} \left(1 - e^{-\frac{\psi\omega}{4}}\right)$$

### A3. Demographic and disease-free equilibrium values

1. Total mouse population constant year-to-year

$$M(t) = M_S(t+1) + M_I(t+1) + M_V(t+1)$$

$$= M_S(t)e^{-\mu} e^{-\frac{\psi\omega}{4}} e^{-\frac{\beta_M}{2} \frac{N_I(t)}{N(t)}} + \frac{\Lambda_M}{4} \left(e^{-\frac{3\mu}{4}} + 3\right)$$

$$+ M_I(t)e^{-\mu} + M_S(t)e^{-\mu} e^{-\frac{\psi\omega}{4}} \left(1 - e^{-\frac{\beta_M}{2} \frac{N_I(t)}{N_S(t)+N_S(t)}}\right)$$

$$+ M_V(t)e^{-\mu} + M_S(t)e^{-\mu} \left(1 - e^{-\frac{\psi\omega}{4}}\right)$$

$$M(t) = e^{-\mu} \left( M(t) + \frac{\Lambda_m}{4} e^{\frac{\mu}{4}} + \frac{3}{4} e^{\mu} \Lambda_M \right)$$

$$\text{Equilibrium solution : } M(t) = \frac{\Lambda_M}{4} \frac{e^{-\frac{3\mu}{4}} + 3}{1 - e^{-\mu}}$$

2. Total nymph population constant year-to-year

$$N(t) = N_S(t+1) + N_I(t+1)$$

$$= \Lambda_T e^{-\frac{(\alpha_1+3\alpha_2)}{4}} \left( e^{-\frac{\beta_L}{4} \frac{M_I(t)e^{-\frac{\mu}{4}} + M_S(t)e^{-\frac{\mu}{4}} e^{-\frac{\psi\omega}{4}} \left(1 - e^{-\frac{\beta_M}{2} \frac{N_I(t)}{N(t)}}\right)}{e^{-\frac{\mu}{4}} [M_I(t) + M_S(t) + M_V(t)] + \frac{\Lambda_M}{4}}} \right)$$

$$+ \Lambda_T e^{-\frac{(\alpha_1+3\alpha_2)}{4}} \left( 1 - e^{-\frac{\beta_L}{4} \frac{M_I(t)e^{-\frac{\mu}{4}} + M_S(t)e^{-\frac{\mu}{4}} e^{-\frac{\psi\omega}{4}} \left(1 - e^{-\frac{\beta_M}{2} \frac{N_I(t)}{N(t)}}\right)}{e^{-\frac{\mu}{4}} [M_I(t) + M_S(t) + M_V(t)] + \frac{\Lambda_M}{4}}} \right)$$

$$= \Lambda_T e^{-\frac{(\alpha_1+3\alpha_2)}{4}}$$

3. Disease-free equilibrium with vaccination

$$N_I(t) = 0$$

$$N_S(t) = \Lambda_T e^{-\frac{(\alpha_1+3\alpha_2)}{4}}$$

$$M_I(t) = 0$$

$$M_S(t) = \frac{\Lambda_M}{4} \frac{\left(e^{-\frac{3\mu}{4}} + 3\right)}{\left(1 - e^{-\mu} - \frac{\psi\omega}{4}\right)}$$

$$M_V(t) = \frac{\Lambda_M}{4} \frac{\left(e^{\frac{\mu}{4}} + 3e^{\mu}\right) \left(1 - e^{-\frac{\psi\omega}{4}}\right)}{\left(-1 + e^{\mu}\right) \left(-1 + e^{\mu} + \frac{\psi\omega}{4}\right)}$$

without vaccination

$$N_I(t) = 0$$

$$N_S(t) = \Lambda_T e^{-\frac{(\alpha_1+3\alpha_2)}{4}}$$

$$M_I(t) = 0$$

$$M_S(t) = \frac{\Lambda_M}{4} \frac{\left(e^{-\frac{3\mu}{4}} + 3\right)}{\left(1 - e^{-\mu}\right)}$$

$$M_V(t) = 0$$

### A4. Derivation of $\mathcal{R}_C$

We begin by decomposing the Jacobian matrix evaluated at the DFE as follows:

$$J = \begin{bmatrix} F + T & \mathcal{O} \\ A & C \end{bmatrix}$$

where  $F + T$  is the  $2 \times 2$  submatrix relating the  $N_I$  and  $M_I$  compartments,  $\mathcal{O}$  is the  $2 \times 1$  zero matrix,  $A$  is a  $1 \times 2$  matrix, and

$C$  is the  $1 \times 1$  matrix  $\left[e^{-\mu - \frac{\psi\omega}{4}}\right]$ .  $F$  consists of all terms relating to new infections and  $T$  consists of all other terms in each matrix entry:

$$F = \begin{bmatrix} \frac{\beta_M \beta_L}{8} \frac{(3e^{-\frac{\mu}{4}} + e^{-\mu})e^{-\frac{\psi\omega}{4}}}{(1-e^{-\mu-\frac{\psi\omega}{4}})} \frac{(1-e^{-\mu})}{(1+3e^{-\mu/4})} & e^{-\mu} \frac{e^{-\frac{(\alpha_1+3\alpha_2)}{4}}(1-e^{-\mu})\beta_L \Lambda_T}{(3e^{-\mu} + e^{-3\mu/4})\Lambda_M} \\ \frac{\beta_M \Lambda_M}{8\Lambda_T} \frac{(3e^{-\frac{\mu}{4}} + e^{-\mu})e^{-\frac{3\mu}{4}-\frac{\psi\omega}{4}}}{(1-e^{-\mu-\frac{\psi\omega}{4}})e^{-\frac{(\alpha_1+3\alpha_2)}{4}}} & 0 \end{bmatrix}$$

and  $T = e^{-\mu} \begin{pmatrix} 0 & 0 \\ 0 & 1 \end{pmatrix}$ .

As with the full Jacobian, the matrix  $F + T$  is singular as well. Let  $F = \begin{pmatrix} ka & kb \\ a & 0 \end{pmatrix}$  and  $T = \begin{pmatrix} 0 & 0 \\ 0 & b \end{pmatrix}$ . We can use these matrices to calculate the next-generation matrix  $Q$  and an expression for  $\mathcal{R}_C$ .

$$Q = F(I_{2 \times 2} - T)^{-1} = \begin{bmatrix} ka & \frac{kb}{1-b} \\ a & 0 \end{bmatrix} \text{ with eigenvalues}$$

$$\lambda_{1,2} = \left\{ \frac{1}{2} \left( ka \pm \sqrt{(ka)^2 + \frac{4(ka)b}{1-b}} \right) \right\},$$

so that

$$\mathcal{R}_C = \frac{1}{2} \left( ka + \sqrt{(ka)^2 + \frac{4(ka)b}{1-b}} \right);$$

since, from (4),  $ka = r(1 - e^{-\mu})$ , this simplifies to

$$\mathcal{R}_C = \frac{1}{2} \left( r(1 - e^{-\mu}) + \sqrt{r^2(1 - e^{-\mu})^2 + 4re^{-\mu}} \right).$$

Since  $e^{-\mu - \frac{\psi\omega}{4}}$ , the spectral radius of  $C$ , is always between 0 and 1,  $\mathcal{R}_C$  provides a stability condition for the disease-free equilibrium. If  $\mathcal{R}_C < 1$ , the equilibrium is stable. Otherwise, it is unstable.

#### A5. Derivation of equilibrium condition

The equilibrium versions of system (3) are as follows:

$$\begin{aligned} M_I^* &= M_I^* e^{-\mu} + (M_\infty - M_V^* - M_I^*) e^{-\mu} e^{-\frac{\psi\omega}{4}} \left( 1 - e^{-\frac{\beta_M}{2} \frac{N_I^*}{N_\infty}} \right) \\ M_V^* &= M_V^* e^{-\mu} + (M_\infty - M_V^* - M_I^*) e^{-\mu} \left( 1 - e^{-\frac{\psi\omega}{4}} \right) \\ N_I^* &= N_\infty \\ &\left( 1 - \exp \left[ -\frac{\beta_L}{4} \frac{M_I^* e^{-\frac{\mu}{4}} + (M_\infty - M_V^* - M_I^*) e^{-\frac{\mu}{4}} e^{-\frac{\psi\omega}{4}} \left( 1 - e^{-\frac{\beta_M}{2} \frac{N_I^*}{N_\infty}} \right)}{e^{-\frac{\mu}{4}} M_\infty + \frac{\Lambda_M}{4}} \right] \right) \end{aligned}$$

Solving the second equation for  $M_V^*$  in terms of  $M_I^*$ .

$$\begin{aligned} M_V^* &= M_V^* e^{-\mu} + (M_\infty - M_V^* - M_I^*) e^{-\mu} \left( 1 - e^{-\frac{\psi\omega}{4}} \right) \\ M_V^*(M_I^*) &= \frac{\left( -1 + e^{\frac{\psi\omega}{4}} \right) (M_\infty - M_I^*)}{\left( -1 + e^{\mu + \frac{\psi\omega}{4}} \right)} \end{aligned}$$

Solving the first equation for  $M_I^*$  in terms of  $N_I^*$ .

$$\begin{aligned} M_I^* &= M_I^* e^{-\mu} + (M_\infty - M_V^* - M_I^*) e^{-\mu} e^{-\frac{\psi\omega}{4}} \left( 1 - e^{-\frac{\beta_M}{2} \frac{N_I^*}{N_\infty}} \right) \\ M_I^*(N_I^*) &= \frac{1 - e^{-\frac{\beta_M}{2} \frac{N_I^*}{N_\infty}}}{e^{\mu + \frac{\psi\omega}{4}} - e^{-\frac{\beta_M}{2} \frac{N_I^*}{N_\infty}}} M_\infty \end{aligned}$$

Solving the third equation in terms of  $N_I^*$ .

$$\begin{aligned} N_I^* &= N_\infty \\ &\left( 1 - \exp \left[ -\frac{\beta_L}{4} \frac{M_I^* e^{-\frac{\mu}{4}} + (M_\infty - M_V^* - M_I^*) e^{-\frac{\mu}{4}} e^{-\frac{\psi\omega}{4}} \left( 1 - e^{-\frac{\beta_M}{2} \frac{N_I^*}{N_\infty}} \right)}{e^{-\frac{\mu}{4}} M_\infty + \frac{\Lambda_M}{4}} \right] \right) \end{aligned}$$

$$G\left(\frac{N_I^*}{N_\infty}\right) = \ln\left(1 - \frac{N_I^*}{N_\infty}\right) + \frac{\beta_L M_\infty e^{-\frac{\mu}{4}} e^{-\frac{\psi\omega}{4}}}{4(e^{-\frac{\mu}{4}} M_\infty + \frac{\Lambda_M}{4})} \left( \frac{1 - e^{-\frac{\beta_M}{2} \frac{N_I^*}{N_\infty}}}{1 - e^{-\mu} e^{-\frac{\psi\omega}{4}} e^{-\frac{\beta_M}{2} \frac{N_I^*}{N_\infty}}} \right) = 0$$

Local stability analysis for the endemic equilibrium using the Jacobian matrix finds that one eigenvalue is zero (as for the disease-free equilibrium), with the other two given by an equation of the form  $\lambda^2 + a_1 \lambda + a_2 = 0$ . Thus by the Jury criterion, the endemic equilibrium is locally asymptotically stable if and only if  $|a_1| < a_2 + 1 < 2$ . In terms of the model parameters, this becomes

$$\begin{aligned} r(1-n) \frac{w^n(1-y^4)(1-y^4z)}{1-y^4zw^n} + y^4(1+zw^n) \\ < r(1-n) \frac{y^4zw^n(1-y^4)(1-y^4z)}{1-y^4zw^n} + y^8zw^n + 1 < 2, \end{aligned}$$

where  $n = N_I^*/N$  obeys  $G(n) = 0$  as in (6),  $w = e^{-\beta_M/2}$ ,  $y = e^{-\mu/4}$ ,  $z = e^{-\psi\omega/4}$ , and  $r$  is as given in Eq. (4). Solving (6) for  $r$  and substituting, the two inequalities simplify to

$$f(n) < \frac{1 - y^4zw^n}{1 - y^4z}, \quad f(n) < \frac{1 - y^8zw^n}{y^4z(1 - y^4)},$$

$$\text{where } f(n) = -\frac{\beta_M}{2}(1-n) \ln(1-n) \frac{w^n}{1-w^n}.$$

One can show that  $0 \leq f(n) \leq 1$  for  $0 \leq n \leq 1$ ,  $0 < w < 1$ , with  $f$  monotone decreasing in  $n$ ,  $f(0) = 1$ ,  $f(1) = 0$  for all  $w \in (0, 1)$ . Meanwhile, the fractions on the right-hand sides of both inequalities are greater than 1 (since  $w, y, z < 1$ ). Thus the Jury criterion is satisfied whenever the endemic equilibrium exists.

#### A6. Parameter estimation

- Calculation of  $\alpha_1, \alpha_2, \alpha_3$ : Using data from literature, we used survival proportions of 0.05, 0.1, and 0.2 between each stage of the tick life cycle (Randolph, 1998) and calculated the  $\alpha$  values based on the proportions of death that we considered in our model.

$\alpha_1$ : Egg to larva

$$\begin{aligned} e^{-\frac{\alpha_1}{4}} &= 0.05 \\ -\frac{\alpha_1}{4} &= \ln(0.05) \\ \alpha_1 &= -4\ln(0.05) \\ &= 11.98/\text{yr} \end{aligned}$$

$\alpha_2$ : Larva to nymph

$$\begin{aligned} e^{-\frac{3\alpha_2}{4}} &= .1 \\ \alpha_2 &= -\frac{4}{3} \ln(0.1) \\ &= 3.07/\text{yr} \end{aligned}$$

$\alpha_3$ : Nymph to adult

$$\begin{aligned} e^{-\frac{\alpha_3}{2}} &= 0.2 \\ \alpha_3 &= 2\ln(0.2) \\ &= 3.22/\text{yr} \end{aligned}$$

- Calculation of  $\mu$ : From literature, we found that the natural death rate of mice was 0.012/day. Thus, we multiplied by 365 to obtain the yearly value of 4.38/year.

- Calculation of  $\Lambda_M$ : Using  $M(t)$  from our equilibrium solution in Appendix A.3 and the chosen value for the total mice population  $M(t) = 50$ , along with  $\mu = 4.38/\text{yr}$ , we have

$$50 = \frac{\Lambda_M}{4} \frac{e^{-\frac{3(4.38)}{4}} + 3}{1 - e^{-4.38}}$$

and thus  $\Lambda_M = 65.02$ .

- Calculation of  $\Lambda_T$ : Using  $N(t)$  from our equilibrium solution in [Appendix A.3](#) and the chosen value for the total nymph population  $N(t) = 1000$ , along with  $\alpha_1 = 11.98/\text{yr}$  and  $\alpha_2 = 3.07/\text{yr}$ , we have

$$1000 = \Lambda_T e^{-\frac{(11.98+3.07)}{4}}$$

and thus  $\Lambda_T = 1.998 \times 10^5$ .

- Estimation of  $\omega$ : We obtained this value from a study that evaluated vaccines in mice, specifically ones that included the same surface protein that we looked into for this study and corresponded with the field trial that we referenced throughout ([Richer et al., 2014](#); [Schwendinger et al., 2013](#)). Though the paper had multiple values for effectiveness, we used the  $\omega$  that corresponded to 100 ng vaccine; this value was presented as a proportion and thus no conversion of units was needed.
- Calculation of  $x$ : The cost of increasing the vaccination rate by 1/day, is estimated by analysis of field data from a vaccine field trial ([Richer et al., 2014](#)). The following data points were used.

#### 1. White-Footed mouse captures

We took data from Table 1: Number of White-Foot Mouse (WFM) Captures in the Field, recreated below.

Study Year	Unique WFM Captured	Nights of Trap Use	Total WFM Captures	WFM Trapability
2007	700	9472	6043	8.63
2008	240	13,824	1647	6.86
2009	716	26,112	5399	7.75
2010	877	27,136	3806	4.83
2011	1258	24,064	6078	4.83
Overall	3791	100,608	22,973	6.48

#### 2. Plots per year

The field trial also used 64 traps per 1.1 hectare plot for distributing vaccines or as controls and used the following number of plots every year.

Year	2007	2008	2009	2010	2011
Plots Used	4	5	7	7	7

Using this data we construct the following equation for bait-box contact rate in a year. Due to the high average captures per mouse we assume that the unique number of mice captured provides a good estimate to the number of mice in all the plots.

$$B(t) = \frac{\text{Total WFM Captures}}{\text{Nights of Trap Use}} * 64 \frac{\text{Number of Plots Used}}{\text{Unique WFM Captured}}$$

We average  $B(t)$  across the five study years to obtain  $B_{\text{Mean}} = .1366$  per day. The study achieved successful vaccination in a mouse after approximately 5 captures so we estimate the study's vaccination rate,  $\psi = \frac{B_{\text{Mean}}}{5} = 0.02732/\text{day} = 9.9718/\text{year}$ . We assume the cost of a bait box distributing vaccine to be equal to a bait box distributing acaricide which are on average priced at \$50 per box per year ([Interlandi, 2018](#)). The cost to vaccinate 1.1 hectares at a rate  $\psi = 9.9718/\text{yr}$  is calculated by  $\frac{\$50 \cdot 64}{\text{year}} = \frac{\$3200}{\text{year}}$ . We then solve for  $x$ :

$$C_{\text{vaccination}} = x * \psi$$

$$3200 = x \cdot 9.718$$

$$x = \$329.29.$$

- Calculation of  $\theta$ : Using values from a study on health care costs of Lyme disease, including Post-Treatment Lyme Disease Syndrome (PTLDS), we used the following equation ([Adrion et al., 2015](#)):

$$\theta = \frac{\text{health care costs}}{\text{for an acute case of Lyme disease}}$$

$$\begin{aligned} & \text{probability of} \\ & \text{developing PTLDS} * \text{average yearly} \\ & \text{cost of PTLDS} \\ & = \$2968 + 0.15(\$3798) \\ & = \$3537.70 \end{aligned}$$

The probability of 0.15 was taken from the same source as an average of the range of probabilities of developing PTLDS (10%-20%).

- Calculation of  $\rho$ : The source cites the probability of Lyme disease after a tick bite to be from 0.012 to 0.05 ([Magid et al., 1992](#)). The center of this range gives 0.031 for our  $\rho$  value.

## References

- Adrion, E.R., Aucott, J., Lemke, K.W., Weiner, J.P., 2015. Health care costs, utilization and patterns of care following Lyme disease. *PLoS One* 10 (2), 1-14.
- Aguilar, S., 2018. *Peromyscus leucopus* white-footed mouse, animal diversity web. [http://animaldiversity.org/accounts/Peromyscus\\_leucopus/](http://animaldiversity.org/accounts/Peromyscus_leucopus/), Accessed: 2018-07-18.
- Allan, B.F., Keesing, F., Ostfeld, R.S., 2003. Effect of forest fragmentation on Lyme disease risk. *Conserv. Biol.* 17 (1), 267-272.
- Allen, L.J.S., van den Driessche, P., 2008. The basic reproduction number in some discrete-time epidemic models. *J. Differ. Equ. Appl.* 14 (11), 1127-1147.
- Barbour, A.G., Bunikis, J., Fish, D., Hanincová, K., 2015. Association between body size and reservoir competence of mammals bearing *Borrelia burgdorferi* at an endemic site in the northeastern united states. *Parasites Vectors* 8 (1), 299.
- Barbour, A.G., Fish, D., 1993. The biological and social phenomenon of Lyme disease. *Science* 260 (5114), 1610-1616.
- Caraco, T., Glavanakov, S., Chen, G., Flaherty, J.E., Ohsumi, T.K., Szymanski, B.K., 2002. Stage-structured infection transmission and a spatial epidemic: a model for Lyme disease. *Am. Nat.* 160 (3), 348-359.
- Centers for Disease Control and Prevention, 2018. Lyme disease. <https://www.cdc.gov/lyme/index.html>.
- Centers for Disease Control and Prevention, 2018. How many people get Lyme disease? <https://www.cdc.gov/lyme/stats/humancases.html>.
- Cook, M.J., 2015. Lyme borreliosis: a review of data on transmission time after tick attachment. *Int. J. Gen. Med.* 8, 1-8.
- Cornstede, P., Shueler, W., Meinke, A., Lundber, U., 2017. The novel Lyme borreliosis vaccine VLA15 shows broad protection against *Borrelia* species expressing six different ospa serotypes. *PLoS One* 10 (9).
- Dobson, A.D.M., Finnie, T.J.R., Randolph, S.E., 2011. A modified matrix model to describe the seasonal population ecology of the European tick *Ixodes ricinus*. *J. Appl. Ecol.* 48 (4), 1017-1028.
- Hersh, M.J., et al., 2014. When is a parasite not a parasite? effects of larval tick burdens on white footed mouse survival. *Ecology* 95 (5), 1360-1369.
- Interlandi, J., 2018. Bait boxes are a safe way to keep ticks out of your yard, Consumer Reports. <https://www.consumerreports.org/pest-control/bait-boxes-are-a-safe-way-to-keep-ticks-out-of-your-yard/>.
- Izac, J.R., Oliver, L.D., Earnhart, C.G., Marconi, R.T., 2017. Identification of a defined linear epitope in the ospa protein of the Lyme disease spirochetes that elicits bactericidal antibody responses: implications for vaccine development. *Vaccine* 35 (25), 3178-3185.
- Jordan, R.A., Schulz, T.L., Jahn, M.B., 2007. Effects of reduced deer density on the abundance of *Ixodes scapularis* (Acar: Ixodidae) and Lyme disease incidence in a northern New Jersey endemic area. *J. Med. Entomol.* 44 (5), 752-757.
- Lane, R.S., Piesman, J., Burgdorfer, W., 1991. Lyme borreliosis: relation of its causative agent to its vectors and hosts in North America and Europe. *Annu. Rev. Entomol.* 36 (1), 587-609.
- LoGiudice, K., Ostfeld, R.S., Schmidt, K.A., Keesing, F., 2003. The ecology of infectious disease: effects of host diversity and community composition on Lyme disease risk. *Proc. Natl. Acad. Sci.* 100 (2), 567-571.
- Magid, D., Schwartz, B., Craft, J., Schwartz, J.S., 1992. Prevention of Lyme disease after tick bites. *New Engl. J. Med.* 327 (8), 534-541.
- Mather, T.N., Telford, S.R., Adler, G.H., 1991. Absence of transplacental transmission of Lyme disease spirochetes from reservoir mice (*Peromyscus leucopus*) to their offspring. *J. Infect. Dis.* 164 (3), 564-567.
- Moreno-Cid, J., de la Lastra J. M., P., et al., 2013. Control of multiple arthropod vector infestations with subolesin/akirin vaccines. *Vaccine* 31 (8), 1187-1196.
- Minnesota Department of Health, 2018. Tickborne diseases. <http://www.health.state.mn.us/divs/idepc/dtopics/tickborne/ticks.html>.
- Nupp, T.E., Swihart, R.K., 1996. Effect of forest patch area on population attributes of white-footed mice (*Peromyscus leucopus*) in fragmented landscapes. *Can. J. Zool.* 74 (3), 467-472.
- Ogden, N.H., Bigras-Poulin, M., O'Callaghan, C.J., Barker, I.K., Kurtenbach, K., Lindsay, L.R., Charron, D.F., 2007. Vector seasonality, host infection dynamics and fitness of pathogens transmitted by the tick *Ixodes scapularis*. *Parasitology* 134 (2), 209-222.
- Ogden, N.H., Bigras-Poulin, M., O'Callaghan, C.J., Barker, I.K., Lindsay, L.R., Maarouf, A., Smoyer-Tomic, K.E., Waltner-Toews, D., Charron, D.F., 2005. A dynamic population model to investigate effects of climate on geographic range and seasonality of the tick *Ixodes scapularis*. *Int. J. Parasitol.* 35 (4), 375-389.
- Ostfeld, R., Brunner, J., 2015. Climate change and *Ixodes* tick-borne diseases of humans. *Philos. Trans. R. Soc. B* 370 (1665), 20140051.

- Ostfeld, R.S., Cepeda, O.M., Hazler, K.R., Miller, M.C., 1995. Ecology of Lyme disease: habitat associations of ticks (*Ixodes scapularis*) in a rural landscape. *Ecol. Appl.* 5 (2), 353–361.
- Ostfeld, R.S., Keesing, F., 2000. Biodiversity and disease risk: the case of Lyme disease. *Conserv. Biol.* 14 (3), 722–728.
- Pugliese, A., Rosa, R., 2008. Effect of host populations on the intensity of ticks and the prevalence of tick-borne pathogens: how to interpret the results of deer exclosure experiments. *Parasitology* 135 (13), 1531–1544.
- Randolph, S.E., 1998. Ticks are not insects: consequences of contrasting vector biology for transmission potential. *Parasitol. Today* 14 (5), 186–192.
- Richer, L.M., Brisson, D., Melo, R., Ostfeld, R.S., Zeidner, N., Gomes-Solecki, M., 2014. Reservoir targeted vaccine against *Borrelia burgdorferi*: a new strategy to prevent Lyme disease transmission. *J. Infect. Dis.* 209 (29), 1972–1980.
- Rosa, R., Pugliese, A., 2007. Effects of tick population dynamics and host densities on the persistence of tick-borne infections. *Math. Biosci.* 208 (1), 216–240.
- Schulze, T., Jordan, R., Williams, M., Dolan, M., 2017. Evaluation of the SELECT tick control system (TCS), a host-targeted bait box, to reduce exposure to *Ixodes scapularis* (Acari: Ixodidae) in a Lyme disease endemic area of New Jersey. *J. Med. Entomol.* 54 (4), 1019–1024.
- Schwan, T.G., Burgdorfer, W., Schrumpf, M.E., Karstens, R.H., 1988. The urinary bladder, a consistent source of *Borrelia burgdorferi* in experimentally infected white-footed mice (*Peromyscus leucopus*). *J. Clin. Microbiol.* 26 (5), 893–895.
- Schwartz, A.M., Hinckley, A.F., Mead, P.S., Hook, S.A., Kugeler, K.J., 2017. Surveillance for Lyme disease United States, 2008–2015. *MMWR Surveill. Summ.* 66 (22), 1–12.
- Schwendinger, M.G., O'Rourke, M., Traweger, A., Savidis-Dacho, H., Pilz, A., Portsmouth, D., Livey, I., Barrett, P.N., Crowe, B.A., 2013. Evaluation of ospA vaccination-induced serological correlates of protection against Lyme borreliosis in a mouse model. *PLoS One* 8 (11), 1–8.
- Shapiro, E.D., 2014. *Borrelia burgdorferi* (Lyme disease). *Pediatrics Rev.* 35 (12), 500–509.
- U.S. Bureau of Labor Statistics, 2019. Consumer price index increased 1.7 percent for year ending september. <https://www.bls.gov/opub/ted/2019/cpi-increased-1-point-7-percent-for-year-ending-september-2019.htm>. Accessed: 2019-10-28.
- Voordouw, M.J., Lachish, S., Dolan, M.C., 2015. The Lyme disease pathogen has no effect on the survival of its rodent reservoir host. *PLoS One* 10 (2).
- Wang, X., Zhao, X.Q., 2017. Dynamics of a time-delayed Lyme disease model with seasonality. *SIAM J. Appl. Dyn. Syst.* 16 (2), 853–881.
- Way, J.G., White, B.N., 2013. Coyotes, red foxes, and the prevalence of Lyme disease. *Northeast. Nat.* 20 (4), 655–665.
- Zhang, Y., Zhao, X.Q., 2013. A reaction-diffusion Lyme disease model with seasonality. *SIAM J. Appl. Math.* 73 (6), 2077–2099.